IOP Publishing Journal of Physics D: Applied Physics

J. Phys. D: Appl. Phys. **47** (2014) 435203 (12pp) doi:10.1088/0022-3727/47/43/435203

# Boltzmann equation and Monte Carlo studies of electron transport in resistive plate chambers

**D Bošnjaković[1,2], Z Lj Petrović[1,2], R D White[3] and S Dujko[1]**

[1] Institute of Physics, University of Belgrade, Pregrevica 118, 11070 Belgrade, Serbia
[2] Faculty of Electrical Engineering, University of Belgrade, Bulevar kralja Aleksandra 73, 11120 Belgrade, Serbia
[3] ARC Centre for Antimatter-Matter Studies, School of Engineering and Physical Sciences, James Cook University, 4811 Townsville, Australia

E-mail: dbosnjak@ipb.ac.rs

Received 18 June 2014, revised 25 August 2014
Accepted for publication 3 September 2014
Published 3 October 2014

**Abstract**

A multi term theory for solving the Boltzmann equation and Monte Carlo simulation technique are used to investigate electron transport in Resistive Plate Chambers (RPCs) that are used for timing and triggering purposes in many high energy physics experiments at CERN and elsewhere. Using cross sections for electron scattering in $C_2H_2F_4$, iso-$C_4H_{10}$ and $SF_6$ as an input in our Boltzmann and Monte Carlo codes, we have calculated data for electron transport as a function of reduced electric field $E/N$ in various $C_2H_2F_4$/iso-$C_4H_{10}$/$SF_6$ gas mixtures used in RPCs in the ALICE, CMS and ATLAS experiments. Emphasis is placed upon the explicit and implicit effects of non-conservative collisions (e.g. electron attachment and/or ionization) on the drift and diffusion. Among many interesting and atypical phenomena induced by the explicit effects of non-conservative collisions, we note the existence of negative differential conductivity (NDC) in the bulk drift velocity component with no indication of any NDC for the flux component in the ALICE timing RPC system. We systematically study the origin and mechanisms for such phenomena as well as the possible physical implications which arise from their explicit inclusion into models of RPCs. Spatially-resolved electron transport properties are calculated using a Monte Carlo simulation technique in order to understand these phenomena.

Keywords: resistive plate chambers, Boltzmann equation, Monte Carlo simulation, electron transport coefficients, negative differential conductivity

(Some figures may appear in colour only in the online journal)

## 1. Introduction

Resistive Plate Chambers (RPCs) are widely used particle detectors due to their simple construction, good detection efficiency, good spatial resolution and excellent timing resolution [1–6]. They are mainly utilized in large high-energy physics experiments for timing and triggering purposes [7–9] but they found their way into applications in other fields, including medical imaging [10, 11] and geophysics [12].

Depending on the applied electric field strength, geometry and gas mixture, RPCs can be operated in avalanche or streamer mode. The avalanche mode of operation provides a much better rate capability than streamer mode, but at the expense of smaller signals [5]. Typical gas mixtures used in the avalanche mode of operation are composed of tetrafluoroethane ($C_2H_2F_4$), iso-butane (iso-$C_4H_{10}$) and sulfur hexafluoride ($SF_6$). Tetrafluoroethane is a weakly electronegative gas with a high primary ionization. Iso-butane is a UV-quencher gas while sulfur hexafluoride is a strongly electronegative gas, used in avalanche mode to suppress the development of streamers. Recently, Abbrescia *et al* [13] have proposed new gaseous mixtures for RPCs that operate in

 

avalanche mode to overcome some of the problems encountered with standard gas mixtures based on tetrafluoroethane, iso-butane and sulfur hexafluoride.

There have been numerous models and simulations of RPCs. Being analytical [14, 15], Monte Carlo [3] or based on fluid equations [16–18], all macroscopic models rely on accurate data for electron swarm transport in gases. These quantities can be either measured in swarm experiments or calculated from electron impact cross sections by the Boltzmann equation analysis or by a Monte Carlo technique [19, 20]. In particle detector community, MAGBOLTZ [21] is the most commonly used Monte Carlo code for such a task. It has been routinely used many times in the past to evaluate electron transport data under the hydrodynamic conditions, and for different experimental arrangements including the Pulsed Townsend (PT) and steady-state Townsend conditions (SST). The motivation for this work lies with the fact that there are some important aspects of electron transport which cannot be analyzed by means of a Monte Carlo method used in MAGBOLTZ. One of these aspects includes the explicit and implicit effects of non-conservative collisions on electron transport and implications which arise from their inclusion in models of RPCs. Collisions in which the number of electrons changes either being produced or removed from the initial ensemble are regarded as non-conservative collisions. Typical examples of these collisions are ionization, attachment, as well as electron-induced detachment from negative ions and electron-ion recombination. These processes may have a marked influence on the electron transport properties and the detector performance. As an illustrative example, Doroud *et al* [22] have shown that the recombination dramatically reduces the amount of charge in the gas filled gap which in turn affects the rate capability in the multi gap RPC used for timing purposes in the ALICE experiment at CERN. In particular, kinetic phenomena induced by the explicit effects of ionization and/or electron attachment should be studied in terms of flux and bulk components of transport coefficients [19, 20, 23]. The distinction between these two sets of transport data has been systematically ignored in the particle detector community and reason for this might be the fact that MAGBOLTZ cannot be used to compute the bulk transport coefficients. At the same time the most accurate experiments used to unfold the cross section data measure bulk coefficients. However, the duality in transport coefficients is easy to understand physically. In this paper we present the required theoretical treatment of the non-conservative corrections, and highlight differences in origin and magnitudes of the bulk and flux transport coefficients for electrons in the gas mixtures used in RPCs in various high energy physics (HEP) experiments at CERN.

Recently, it was shown that the addition of $SF_6$ (and iso-$C_4H_{10}$) to standard RPC mixtures may improve several important aspects of the RPC performance in avalanche mode, including efficiency and time resolution [24]. It has been long established that electron attachment to $SF_6$ leads to the formation of both parent ($SF_6^-$) and fragment ($SF_5^-$, $SF_4^-$, $SF_3^-$, $SF_2^-$, $F_2^-$ and $F^-$) negative ions [25]. In particular, the cross section for the creation of stable parent negative ions $SF_6^-$ at zero energy is huge suggesting that the lower energy electrons are most likely to be consumed before their recombination with the positive ions. This in turn may induce some attachment induced kinetic phenomena in electron transport due to the strong electronegative nature of $SF_6$. One of the most striking phenomena induced by strong electron attachment in the mixtures of rare gases and fluorine is the negative absolute electron mobility [26, 27]. Occurrence of these phenomena should be carefully considered in numerical simulations in accordance with the experimental evaluation of the RPC performance.

Here we do not attempt to consider primary ionization effects, space charge effects and signal induction in the presence of resistive material nor do we attempt to compute the RPC performances, i.e. efficiency, time resolution and charge spectra. These important elements of modeling are the subject of our future publications [28]. Instead we isolate and investigate electron swarms under the action of a spatially uniform electric field. In the present work we solve the Boltzmann equation for electrons undergoing non-conservative collisions in the gas mixtures of $C_2H_2F_4$, iso-$C_4H_{10}$ and $SF_6$ used in RPCs in various HEP experiments at CERN. In this application electron attachment and ionization play a key role in the electron behavior, therefore any modeling must treat them in a comprehensive manner. Variation and general trends of the mean energy and effective ionization coefficient, drift velocity and diffusion tensor with the applied reduced electric field are presented. We use our Monte Carlo simulation technique as a complementary method to Boltzmann's equation with the specific purpose to evaluate the spatially resolved transport data and distribution functions amidst non-conservative collisions. The knowledge of spatially resolved transport data is very useful in modeling of RPCs and understanding their performance. Fluid models of RPCs can be further improved by considering the non-local effects induced by a large spatial variation in the electric field during the avalanche-streamer transition or due to presence of physical boundaries. Correct implementation of transport data and accuracy of their calculation is also highlighted in the present work. Our methodology based on complementary Boltzmann and Monte Carlo studies of electron transport in neutral gases has already been used in different gas discharge problems [29]. This is the first paper to our knowledge where the combined Boltzmann equation analysis and Monte Carlo simulation technique are applied to the description of electron kinetics in the gas mixtures used in RPCs.

This paper is organized as follows. In section 2 we substantiate the existence of hydrodynamic regime and identify the differences in the bulk and flux transport coefficients. In section 2.1 we give a brief discussion of the theoretical multi term solution of the Boltzmann equation under non-conservative conditions. The basic elements of our Monte Carlo simulation code are discussed in section 2.2. In section 3, we present the results of a systematic study of electron transport in the gas mixtures used in RPCs that are used for timing and triggering purposes in many high energy experiments at CERN. We focus on the way in which the transport coefficients are influenced by non-conservative collisions, particularly by electron attachment. Spatially resolved energy and rate coefficients as well as spatial profiles of the electrons are calculated

by a Monte Carlo simulation technique with the aim of understanding the NDC and related phenomena. This paper represents the first comprehensive treatment of non-conservative electron transport in typical RPC gas mixtures based on a rigorous Boltzmann equation analysis and the Monte Carlo simulation technique.

## 2. Theoretical methods

Electron transport in non-conservative RPC gases should be analyzed in terms of bulk (e.g. reactive) and flux components. The main motivation for such analysis is to gain insight into the effect of non-conservative processes on electron transport as these processes influence many operating characteristics of the detector. For example, there is a direct link between the effective ionization coefficient and time resolution of an RPC. Spatial resolution, on the other hand, is greatly affected by transverse diffusion while the role of attachment processes is twofold. On one hand, electron attachment is a desirable process as it controls the avalanche multiplication and limits the amount of charge between the electrodes, which in turns improves the rate capability of an RPC. On the other hand, if the attachment is too strong with a large exponential decay rate for electrons then the time resolution and efficiency might be seriously affected. It is clear that care must be taken when non-conservative collisions are operative to ensure the optimal performance of the detector.

### 2.1. A brief sketch of the Boltzmann equation analysis

All information on the drift and diffusion of electrons in gases is contained in the electron phase-space distribution function $f(\mathbf{c}, \mathbf{r}, t)$, where $\mathbf{r}$ represents the spatial coordinate of an electron at time $t$, and $\mathbf{c}$ denotes its velocity. The distribution function $f(\mathbf{r}, \mathbf{c}, t)$ is evaluated by solving Boltzmann's equation:

$$\left(\partial_t + \mathbf{c}\cdot\nabla_{\mathbf{r}} + \frac{\mathrm{e}}{m}\mathbf{E}\cdot\nabla_{\mathbf{c}}\right) f(\mathbf{r}, \mathbf{c}, t) = -J(f, f_0) \ , \tag{1}$$

where $\partial_t$, $\nabla_{\mathbf{r}}$ and $\nabla_{\mathbf{c}}$ are the gradients with respect to time, space and velocity, while e and $m$ are the charge and mass of the electron and $\mathbf{E}$ is the magnitude of the electric field. The right-hand side of (1) $J(f, f_0)$ denotes the linear electron-neutral molecule collision operator, accounting for elastic, inelastic and non-conservative (e.g. electron attachment and/or ionization) collisions, and $f_0$ is the velocity distribution function of the neutral gas (usually taken to be Maxwellian at fixed temperature). For elastic collisions we use the original Boltzmann collision operator [30], while for inelastic collisions we prefer the semiclassical generalization of Wang-Chang *et al* [31]. The collision operators for non-conservative collisions are discussed in [32, 33]. We assume that in the division of post-collision energy between the scattered and ejected electrons in an ionization process, all fractions are equally probable.

Solution of Boltzmann's equation (1) has been extensively discussed in our recent reviews [20, 34]. In brief, $f$ is expanded in terms of normalized Burnett functions about a Maxwellian at an arbitrary temperature $T_\mathrm{b}$. In the hydrodynamic regime, its space-time dependence is expressed by an expansion in terms of the gradient of the electron number density $n(\mathbf{r}, t)$. This assumption is generally valid for an RPC detector even in the regions where high energy particle creates the clusters of electrons with steep density gradients. One may expect that diffusion processes will act to validate the assumption on weak gradients after a certain period of time. Thus, the following expansion of the phase-space distribution function follows:

$$f(\mathbf{r}, \mathbf{c}, t) = \widetilde{\omega}(\alpha, c) \sum_{\nu=0}^{\infty} \sum_{l=0}^{\infty} \sum_{m=-l}^{l} \sum_{s=0}^{\infty} \sum_{\lambda=0}^{s} F(\nu lm|s\lambda;\alpha)\, \phi_m^{[\nu l]} G_m^{(s\lambda)} n(\mathbf{r}, t) \ , \tag{2}$$

where

$$\widetilde{\omega}(\alpha, c) = \left(\frac{\alpha^2}{2\pi}\right)^{3/2} \exp\left(-\frac{\alpha^2 c^2}{2}\right), \tag{3}$$

is a Maxwellian distribution function at a temperature $T_\mathrm{b}$, with $\alpha^2 = \dfrac{m}{kT_\mathrm{b}}$. $T_\mathrm{b}$ is not equal to the neutral gas temperature and serves as a free and flexible parameter to optimize the convergence. The quantities $\phi_m^{[\nu l]}$ and $G_m^{(s\lambda)}$ are normalized Burnett functions and irreducible gradient tensor operator, respectively, and are defined in [32, 33]. The coefficients $F(\nu lm|s\lambda;\alpha)$ are called 'moments' and are related to the electron transport properties as detailed below. The bulk drift velocity ($W$), bulk diffusion coefficients ($D_L$, $D_T$) and effective ionization coefficient ($k_{\mathrm{eff\ ion}}$) are defined in terms of the diffusion equation and can expressed in terms of moments as follows [20, 34]:

$$W = \frac{\mathrm{i}}{\alpha} F(010|00) - \mathrm{i}n_0 \sum_{\nu'=1}^{\infty} J_{0\nu'}^0(\alpha)\, F(\nu'00|11) \ , \tag{4}$$

$$D_L = -\frac{1}{\alpha} F(010|11) - n_0 \left( \sum_{\nu'=1}^{\infty} J_{0\nu'}^0(\alpha)\, F(\nu'00|20) - \sqrt{2}\, F(\nu'00|20) \right), \tag{5}$$

$$D_T = -\frac{1}{\alpha} F(011|11) - n_0 \left( \sum_{\nu'=1}^{\infty} J_{0\nu'}^0(\alpha)\, F(\nu'00|20) + \frac{1}{\sqrt{2}} F(\nu'00|22) \right), \tag{6}$$

$$k_{\mathrm{eff\ ion}} = \mathrm{i}n_0 \sum_{\nu'=1}^{\infty} J_{0\nu'}^0(\alpha)\, F(\nu'00|00) \ , \tag{7}$$

where $J_{0\nu'}^0(\alpha)$ are reduced matrix elements of the collision operator. The bulk transport coefficients are the sum of the flux transport coefficients (defined in terms of Fick's law and given the first terms in each of the expressions (4)–(6)) and a contribution due to non-conservative collisions (the terms involving the summations in each expression). Differences between the two sets of coefficients thus arise when non-conservative processes are operative. The reader is referred to

[19, 20, 23, 34] for full details. Also of interest is the spatially homogeneous mean energy

$$\varepsilon = \frac{3}{2}kT_{\mathrm{b}}\left(1 - \sqrt{\frac{2}{3}}F\left(100|00\right)\right). \tag{8}$$

Using the above decomposition of $f$ (2), the Boltzmann equation (1) is converted to a hierarchy of doubly infinite set of coupled algebraic equations for the moments. To obtain electron transport coefficients identified in (4)–(6) under conditions when the transport is greatly affected by non-conservative collisions, the index $s$ in (2) must span the range (0–2) (e.g. second-order density gradient expansion). Solution of the system of equations can be found by truncation of the infinite summations in the velocity space representation in (2) at $l_{\max}$ and $\nu_{\max}$, respectively. The values of these indices required to achieve the designated convergence criterion, represent respectively the deviation of the velocity distribution from isotropy in velocity space, and the deviation from a Maxwellian speed distribution at the basis temperature $T_{\mathrm{b}}$. The classical two term approximation sets $l_{\max} = 1$, which is not sufficient for molecular gases used in an RPC due to the anisotropy of $f$ in velocity space. A value of $l_{\max} = 5$ was required for achieving an accuracy to within 1% . Depending of the basis temperature, values of $\nu_{\max} = 95$ were sometimes required under conditions when the distribution function was strongly non-equilibrium and far away from a Maxwellian. The resulting coefficient matrix is sparse and direct numerical inversion procedure is used to calculate the moments.

One should be aware of the differences in the definition of both sets of transport data, bulk and flux, and make sure that proper data are employed in the models. MAGBOLTZ is routinely used in particle detector community for determination of electron transport properties and few comments about this code are appropriate here. MAGBOLTZ cannot compute the bulk transport coefficients and it is exactly these data that are required for some aspects of modeling. For example, in the application of Legler's model for the avalanche size distribution as a function of the distance [2, 35], one should use the bulk drift velocity to evaluate the ionization coefficient. In addition, the bulk data should be generally used to unfold cross sections from experimentally measured and theoretically calculated transport coefficients [19, 20]. On the other, in fluid modeling of RPCs [16–18] the flux data should be generally used as an input although in some combined fluid/Monte Carlo models the bulk data are required. Generally speaking, the distinction between the bulk and flux data has been systematically ignored in the particle detector community and one of the principal aims of this work is to sound a warning to those who implement the swarm data to be aware of the origin of the transport data and the type of transport data required in their modeling. In this paper we illustrate that bulk and flux data may exhibit not only quantitative but also the qualitative differences in the mixtures of $C_2H_2F_4$, iso-$C_4H_{10}$ and $SF_6$ used in RPCs operated in avalanche mode.

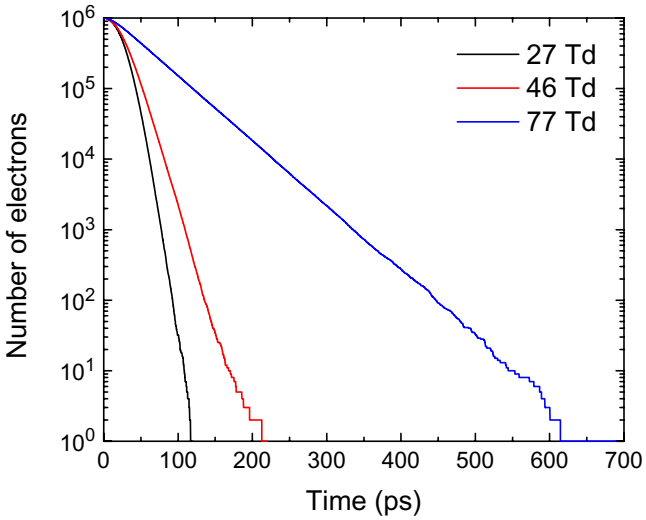


**Figure 1.** Exponential decay of the number of electrons for three different reduced electric fields as indicated on the graph. Calculations are performed for electrons in ALICE TOF RPC system.

### *2.2. A brief overview of our Monte Carlo simulation technique*

Rather than present a full review of our Monte Carlo simulation technique, we highlight below some of its aspects associated with the sampling of spatially resolved electron transport data. In this work we apply the code primarily to calculate spatially resolved transport data with an aim of using these data to understand the sometimes atypical manifestations of the drift and diffusion in the RPCs. In order to sample spatially resolved transport parameters under hydrodynamic conditions, we have restricted the space to realistic dimensions of the RPC and divided it into cells. Every cell contains 100 sub-cells and these sub-cells are used to sample spatial parameters of electron swarm. This concept allowed us to follow the development of the swarm in both real space and normalized to $6\sigma$, where $\sigma$ is the standard deviation of the Gaussian distribution in space. The space (and time) resolved electron transport properties including the average energy/velocity and rate coefficients and also density profiles have been determined by counting the electrons and their energies/velocities as well as number of collisions in every cell.

When electron transport is greatly affected by non-conservative collisions, it is of key importance for a tractable simulation to efficiently control the number of electrons in simulations without distortion of the spatial gradients of the distribution function. It is well known that the statistical uncertainty of a Monte Carlo simulation decreases inversely with the square root of the number of electrons processed. In particular, when attachment occurs, electrons are lost continually, so that the number of electrons in the swarm decreases exponentially with time. This is illustrated in figure 1 for electrons in the gas mixture used in ALICE timing RPC.

The initial number of electrons is set to $1 \times 10^6$ and calculations are performed for a range of reduced electric fields $E/N$ as indicated on the graph. We see that as $E/N$ decreases the number of electrons decreases markedly. This is a consequence of an increasing collision frequency for electron attachment when $E/N$ is reduced. In order to compensate

the electrons that are consumed by a strong attachment at low electron energy, the following rescaling procedure was adopted. First, the sampling time used for determination of various swarm dynamic properties (for example the mean position, velocity and energy of the electrons) was reduced and adjusted depending on the applied reduced electric field. Second, whenever electron is lost due to attachment another electron is randomly selected in its place from the ensemble of the remaining electrons. This was necessary in order to prevent large and continuous losses of electrons. This procedure was validated for a range of model and real gases when attachment is dominant non-conservative process and found to be correct [36, 37]. Other rescaling procedures to electron swarms with large exponential decay rates are available. The classical example is the procedure developed by Li *et al* [38]. The essence of their rescaling procedure is the addition of an artificial ionization channel with an energy-independent ionization frequency, chosen to be roughly equal to an attachment collision frequency for a given *E*/*N*. Similar procedure was applied to simulate electron transport in pure $SF_6$ by Yousfi *et al* [39]. Finally, we note that when ionization takes place the rescaling procedure was not necessary under conditions considered in this work, as ionization was not a sufficiently intensive process to increase the number of electrons beyond the limits set by the allocated memory.

## 3. Results and discussion

### 3.1. Preliminaries

As discussed in section 1, one of the aims of this work is to consider electron transport parameters as input in fluid and kinetic models of RPCs. The operating values of *E*/*N* for RPCs are above the critical electric fields for the corresponding gas mixtures, usually between 400 Td and 450 Td for timing RPC depending on the type of experiment and around 200 Td for triggering RPC. Fluid models of these detectors in both avalanche and streamer modes, however, require tabulation of transport data over a wide range of the reduced electric fields and/or mean energy of the electrons depending on the order of fluid approach [40, 41]. In this work we consider the reduced electric field range: 1–1000 Td (1Td = $1 \times 10^{-21}$ $Vm^2$) while the pressure and temperature of the background gas are 1 atm and 293 K, respectively.

The cross sections for electron scattering from $C_2H_2F_4$ detailed in Šašić *et al* [42] are used in this study. The cross sections for electron scattering in iso-$C_4H_{10}$ are taken from MAGBOLTZ code developed by Biagi. Finally, the cross sections for electron scattering in $SF_6$ are taken from Itoh *et al* [43]. Other sets of cross sections for electron scattering in these gases are available in the literature but our Boltzmann equation analysis has revealed that the present sets provide values of swarm parameters such as ionization and electron attachment rate coefficients, drift velocity, longitudinal and transverse diffusion coefficient in a good agreement with the experimental measurements for a wide range of *E*/*N* [44, 45]. The following mixtures are used for different RPCs considered in this work: (1) ALICE timing RPC $C_2H_2F_4$/iso-$C_4H_{10}$/$SF_6$ = 90/5/5 [8]; (2) ALICE triggering RPC $C_2H_2F_4$/iso-$C_4H_{10}$/$SF_6$ = 89.7/10/0.3 [8]; (3) CMS triggering RPC $C_2H_2F_4$/iso-$C_4H_{10}$/$SF_6$ = 96.2/3.5/0.3 [9]; and (4) ATLAS triggering RPC $C_2H_2F_4$/iso-$C_4H_{10}$/$SF_6$ = 94.7/5/0.3 [7].

### 3.2. Effects of non-conservative collisions

In the following sections we often find it necessary to refer to the explicit influence of electron attachment and/or ionization on electron transport to explain certain phenomena. The following elementary considerations apply. Even under the hydrodynamic conditions (far away from the boundaries, sources and sinks of electrons) the distribution of the average energy within the swarm is spatially anisotropic. This is illustrated in section 3.3 where spatially resolved average energy for electrons in ALICE timing RPC is shown as a function of *E*/*N*. Electrons at the front of the swarm generally have higher energy than those at the trailing edge, as on the average they have been accelerated through a larger potential. Since electron attachment and ionization are energy dependent, they will also occur with a spatial dependence. For example, if the collision frequency for electron attachment increases with energy, attachment will predominantly occur at the front of the swarm, resulting in a backwards shift of the swarm's centre of mass, which is observable as a reduction of the bulk drift velocity as compared with the flux drift velocity. The loss of high energy electrons also lowers the mean energy which in turns reduces the flux component of the diffusion. This process is known as *attachment cooling* [33].

If the collision frequency for electron attachment decreases with energy, then the opposite situation holds: the lower energy electrons at the trailing edge of the swarms will be consumed resulting in a forward shift of the swarm's centre of mass, which is observable as an increase of the bulk drift velocity. The mean energy is raised as the lower energy electrons are consumed resulting in an enhancement of the flux components of transverse and longitudinal diffusion. This phenomenon is known as *attachment heating* [32] and is particularly important for electron transport in the gas mixtures used in RPCs. Finally, when ionization takes place, electrons are preferentially created in regions of higher energy resulting in a shift in the centre of mass position as well as a modification of the spread about the centre of mass. This will be observable as an increase of the bulk drift velocity and the bulk diffusion coefficients. This situation also plays an important role in consideration of electron kinetics in RPCs analyzed in this work.

### 3.3. Boltzmann equation results for electron transport coefficients

In figure 2 we show the variation of mean energy with *E*/*N* for RPCs used in ALICE, CMS and ATLAS experiments at CERN.

The properties of the cross sections are reflected in the profiles of the mean energy and we observe three distinct regions of transport. Excepting ALICE timing RPC, in the remaining experiments we first observe a region of slow rise due to (relatively) large energy losses associated with vibrational

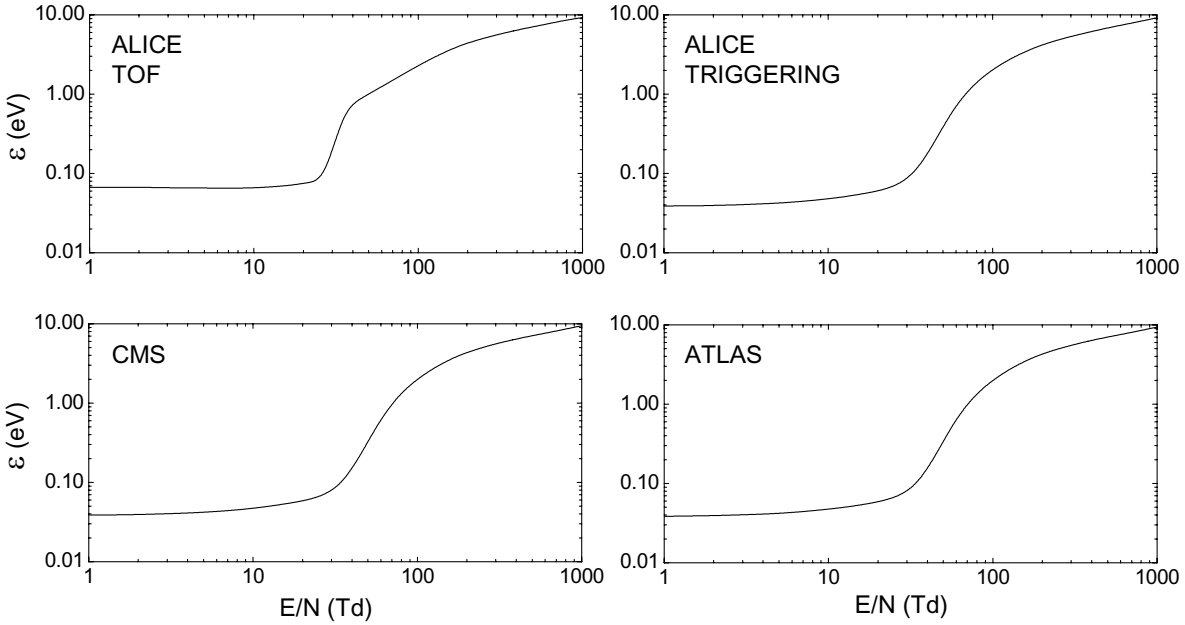


**Figure 2.** Variation of the mean energy with *E*/*N* for RPCs used in ALICE, CMS and ATLAS experiments at CERN.

excitations. Second, there is a region of sharp rise as the cross sections for vibrational excitations drop off and electrons start to gain energy from the electric field rapidly. Finally, there is another region of slow rise in the mean energy as new inelastic channels including the electronic excitation, neutral dissociation and ionization become open. The variation of the mean energy with *E*/*N* in these three RPCs systems is almost identical due to small differences in the abundances of $C_2H_2F_4$ and iso-$C_4H_{10}$ in the gas mixtures. The amount of $SF_6$ in these systems is the same and set to 0.3%.

However, for ALICE timing RPC the situation is more interesting. In this system the amount of $SF_6$ in the gas mixture is much higher and the electron transport is greatly affected by electron attachment. In the limit of the lowest *E*/*N* considered in this work (less than 10 Td) and contrary to the results for other RPC systems, we see that for increasing *E*/*N* the mean energy varies very slowly and essentially stays unaltered. We also observe that the mean energy is significantly higher than thermal electron energy $\left(\frac{3}{2}kT\right)$ indicating the presence of an additional heating mechanism for electrons. This unusual situation follows from the combined effects of attachment heating and inelastic cooling. The term *inelastic cooling* simply refers to the fact that whenever an electron undergoes an inelastic collision it loses at least the threshold energy of the excitation process and emerges from the collision with reduced energy. In the energy range of interest, the collision frequency for electron attachment (which leads to the formation of stable parent $SF_6^-$ negative ion) decreases with the electron energy and the lower energy electrons which predominantly exist at the trailing edge of the swarm are preferentially consumed. As already discussed in section 3.2, under these conditions the mean energy is raised and bulk drift velocity is increased (see figure 3). However, due to inelastic cooling if the electrons have energy just above the threshold energy, then in any inelastic encounter with a neutral they will lose almost all energy, resulting in a substantial cooling effect on the swarm, even if only a relatively small fraction of the electrons have the required energy. This is exactly what happens for electrons in ALICE timing RPC; due to attachment heating the mean energy is raised above thermal energy and due to inelastic cooling the mean energy cannot be further increased for increasing *E*/*N* as the collision frequency for inelastic collisions in this energy range rapidly increases with the electron energy.

In figure 3 we show the variation of the bulk and flux drift velocity with *E*/*N* for RPCs used in ALICE, CMS and ATLAS experiments at CERN. In all experiments the bulk component dominates the flux component over the entire *E*/*N* range consider in this work. For lower *E*/*N* this follows from the attachment heating while for higher *E*/*N* this is a consequence of the explicit effects of ionization on the drift velocity. The effects of electron attachment are stronger than those induced by ionization and are the most evident for ALICE timing RPC where differences between the bulk and flux values are of the order of 100% for lower *E*/*N*. For other RPC systems these differences are of the order of 10% for lower *E*/*N* while for higher *E*/*N* are around 20%.

The existence of negative differential conductivity (NDC) in the bulk drift velocity component with no indication of any NDC for the flux component in the ALICE timing RPC system is certainly one of the most striking phenomena observed in this work. NDC is a kinetic phenomenon which represents the decrease of the drift velocity with increasing driving electric field. From the plot of the drift velocity for ALICE timing RPC it is seen that electrons exhibit NDC in the bulk drift velocity for reduced electric fields between 30 Td and 100 Td. Conditions leading to this phenomenon have been extensively discussed by Petrović *et al* [46] and Robson [47]. In brief, it was concluded that NDC arise from certain combination of

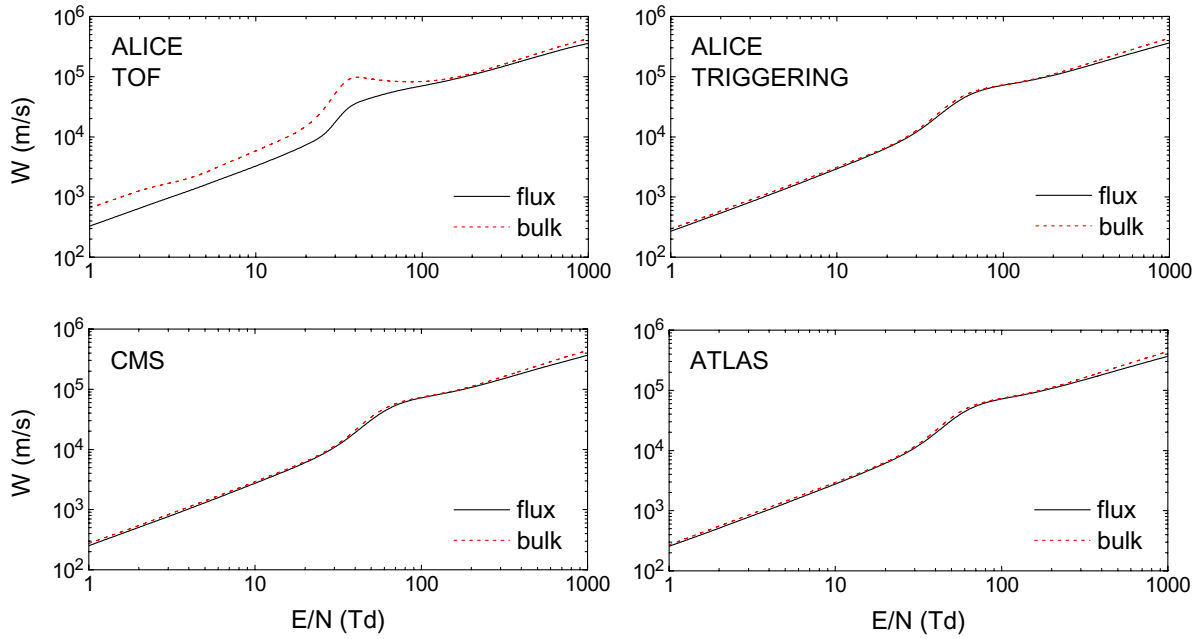


**Figure 3.** Variation of the bulk and flux drift velocities with *E*/*N* for RPCs used in ALICE, CMS and ATLAS experiments at CERN.

elastic-inelastic cross sections and is present in both the bulk and flux drift velocity components. The conditions for the attachment or ionization (non-conservative collision) induced NDC were first discussed by Vrhovac and Petrović [48] where it was concluded that the effect is possible but most likely to result in both bulk and flux drift velocities albeit at a different degree. This paper left a possibility that the flux drift velocity may not have NDC but a strongly developed plateau indicating that the NDC is on verge of being observable. This conclusion was based on the survey of observable effects for most gases with strong dissociative attachment.

In our case, however, NDC is present only in the bulk drift velocity which is a reminiscent of recently observed NDC effect for positrons in molecular gases [49, 50]. In these studies, it was concluded that NDC is induced by non-conservative nature of Positronium (Ps) formation. This conclusion has been confirmed in calculations where the Ps formation was treated as a conservative inelastic process; the NDC phenomenon has been removed from the profiles of the bulk drift velocity along with the differences between bulk and flux drift velocity components. Following the same strategy, we have treated electron attachment as a conservative inelastic process for $SF_6$ in our Boltzmann equation analysis. Results of our calculations are shown in figure 4. We see that NDC is absent from the profile of the bulk drift velocity and the only differences between the bulk and flux drift velocity are those originating from the explicit contribution of ionization for *E*/*N* higher than approximately 200 Td. The physical mechanisms behind the attachment induced NDC phenomenon is discussed in section 3.4.

In figures 5 and 6 we show the variation of the longitudinal and transverse diffusion coefficients with *E*/*N* for RPCs used in ALICE, CMS and ATLAS experiments at CERN. Both the bulk and flux values are shown and we see that all diffusion

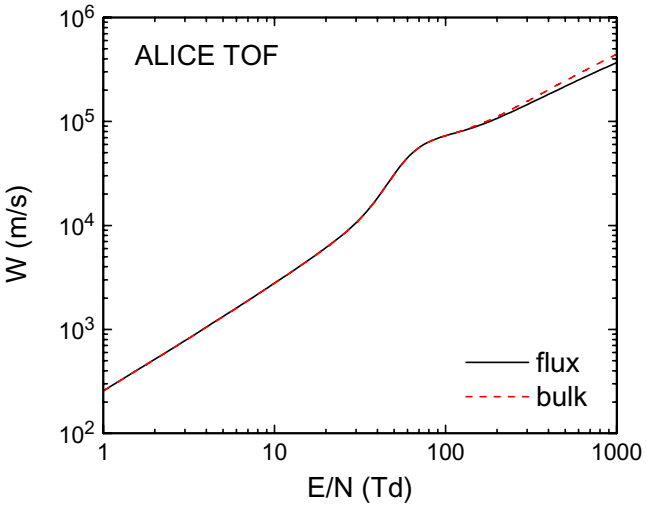


**Figure 4.** Variation of the bulk and flux drift velocity with *E*/*N* when electron attachment is treated as a conservative inelastic process for electrons in an ALICE timing RPC.

coefficients reflect to some degree the three distinct regions of electron transport discussed above. For ALICE triggering, CMS and ATLAS RPC systems, the variations of bulk and flux components of $ND_L$ and $ND_T$ with *E*/*N* are almost identical. Differences between the bulk and flux data for $ND_L$ and $ND_T$ are of the order of 20% . In these systems the differences between the bulk and flux values are only of quantitative nature and are not as high as those present between the bulk and flux values for $ND_L$ and $ND_T$ in the ALICE timing RPC system. In this case the bulk and flux components of the diffusion coefficients exhibit *qualitatively* different behavior; although as *E*/*N* increases both $ND_L$ and $ND_T$ generally increase, there exist certain regions of *E*/*N* where the bulk components of both $ND_L$ and $ND_T$ (and flux $ND_L$) are decreased for increasing *E*/*N*.

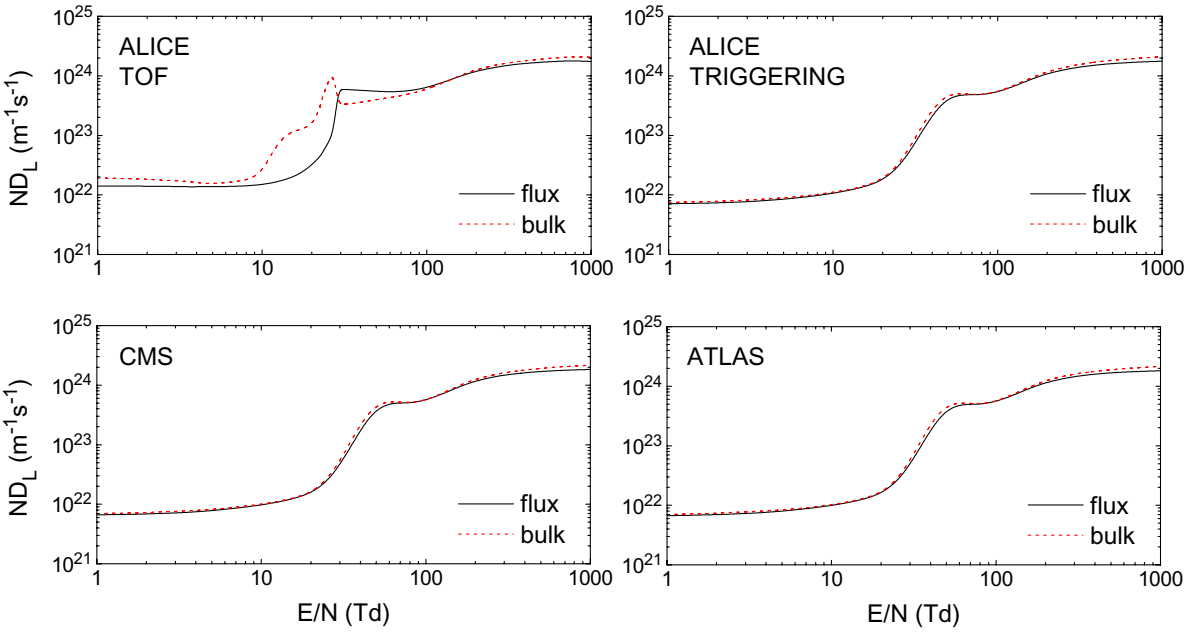


**Figure 5.** Variation of the longitudinal diffusion coefficient with *E*/*N* for RPCs used in ALICE, CMS and ATLAS experiments at CERN. Dashed lines are bulk coefficients while solid lines represent flux coefficients.

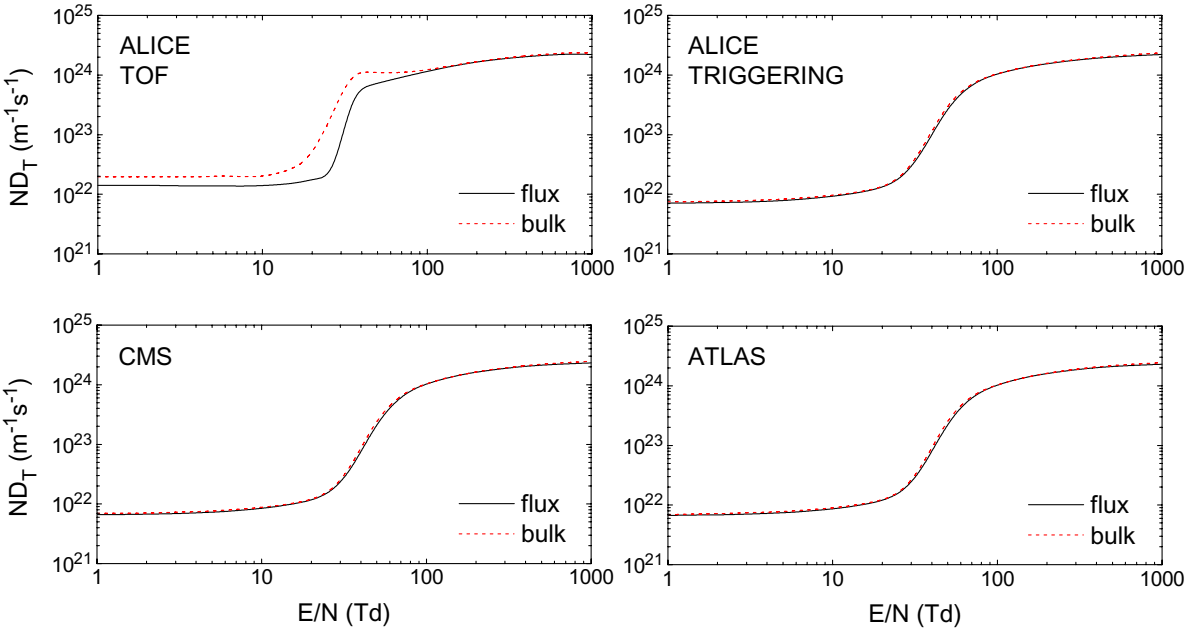


**Figure 6.** Variation of the transverse diffusion coefficient with *E*/*N* for RPCs used in ALICE, CMS and ATLAS experiments at CERN. Dashed lines are bulk coefficients while solid lines represent flux coefficients.

This illustrates the complexity of diffusion processes in general and for electrons in RPC systems at CERN indicating how difficult it is to understand the influence of non-conservative collisions on the diffusion coefficients. In brief, many parallel factors affect the diffusion simultaneously. In addition to the effects of thermal anisotropy (dispersion of electrons due to thermal motion is not the same in different directions) and anisotropy at elevated reduced electric fields (spatial variation of the average energy in conjunction with energy-dependent collision frequency produces differences in the average local velocities for a given direction, which act to inhibit and/or enhance diffusion in that direction), there is always the contribution of non-conservative collisions and the complex energy dependence of electron attachment and ionization that even further complicate the physical picture. In conclusion, our results suggest a weak sensitivity of the diffusion coefficients with respect to electron attachment and ionization for ALICE triggering, CMS and ATLAS RPC systems and a much more complex behavior of diffusion processes for electrons in ALICE timing RPC.

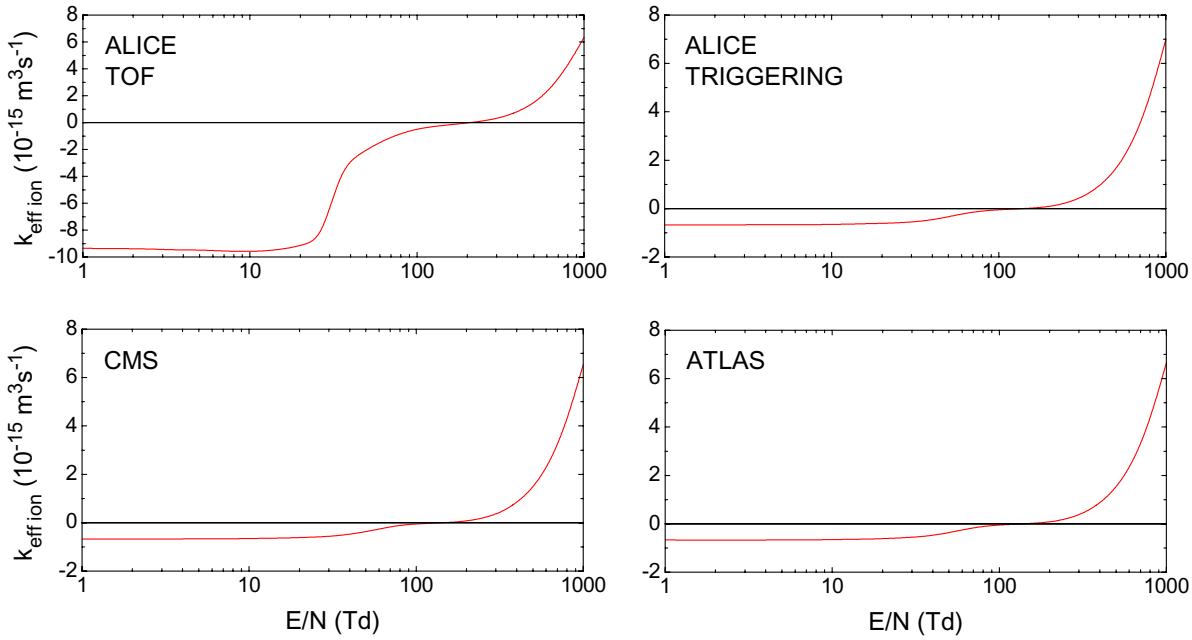


**Figure 7.** Variation of the effective ionization coefficient with *E*/*N* for RPCs used in ALICE, CMS and ATLAS experiments at CERN.

In figure 7 we show the variation of the effective ionization coefficient with *E*/*N* for RPCs used in ALICE, CMS and ATLAS experiments at CERN. The variation of this property with *E*/*N* is almost identical for ALICE triggering, CMS and ATLAS RPC systems due to small variations in the abundances of $C_2H_2F_4$ and iso-$C_4H_{10}$ in the gas mixtures. The critical electric field for these systems is around 140 Td. The critical electric field for ALICE timing RPC is much higher, around 215 Td, due to higher abundance of $SF_6$ in the gas mixture and stronger effects of electron attachment on the electron energy distribution function.

### *3.4. Monte Carlo results for spatially resolved transport data and distribution function*

While all results presented above may reproduced exactly (for all practical purposes) by Monte Carlo simulation (albeit with a much more computing effort) there is a number of results important for RPC modeling that may be obtained by Monte Carlo technique with less difficulty and a more direct interpretation. In this section we show spatially resolved electron transport data that are sampled at every location over the entire swarm. The effect of the electric field on the spatial distribution of the electron transport data and distribution function is examined. In figure 8 we show the spatial profile and spatially resolved average energy for four different values of *E*/*N* as indicated in the graphs. The Monte Carlo simulations were simplified by assuming stationary gas ($T$ = 0 K). This is the reason why our Monte Carlo results for electron transport coefficients are slightly shifted to the left, towards lower *E*/*N* comparing to our Boltzmann equation results obtained for the gas temperature of 293 K (not shown here). As a consequence, according to our Monte Carlo simulations the NDC occurs approximately between 20 Td and 77 Td while the Boltzmann equation analysis suggest the NDC between 30 Td and 100 Td. One should bear this in mind in the following discussions.

In addition to our actual results given by solid lines where electron attachment is treated as a true non-conservative process, the results denoted by the dashed lines are obtained assuming electron attachment as a conservative inelastic process with zero energy loss. When electron attachment is treated as a conservative inelastic process, the spatial profile of electrons is almost perfectly symmetric and it has a typical Gaussian profile independently of the applied *E*/*N*. The spatially resolved average energy has a characteristic slope indicating spatially anisotropic distribution of the electron energy. There are no imprinted oscillations in the spatial profile of the electrons or in the profile of the average energy indicating the collisional energy loss is governed essentially by 'continuous' energy loss processes [51].

When electron attachment is treated regularly, as a true non-conservative process, we observe dramatic modifications to the spatial profile of the electron density and to the spatially resolved average energy. For *E*/*N* of 5.9 Td and 10 Td the spatial profile of electrons is no longer Gaussian while for *E*/*N* of 21 Td the spatial profile exhibits an asymmetric Gaussian distribution whose height is significantly decreased comparing to the Gaussian profile of the swarm when electron attachment is treated as a conservative inelastic process. For *E*/*N* = 5.9 Td we see that the average energy is essentially spatially uniform along the swarm. This is indicative of our normalization procedure: the spatial profile is not symmetric and number of electrons attachments is also asymmetric along the swarm and combination of these two yields a little spatial variation of the average energy along the swarm. For *E*/*N* = 10 Td, however, we observe that the trailing edge of the swarm is drastically cut off while the average energy remains

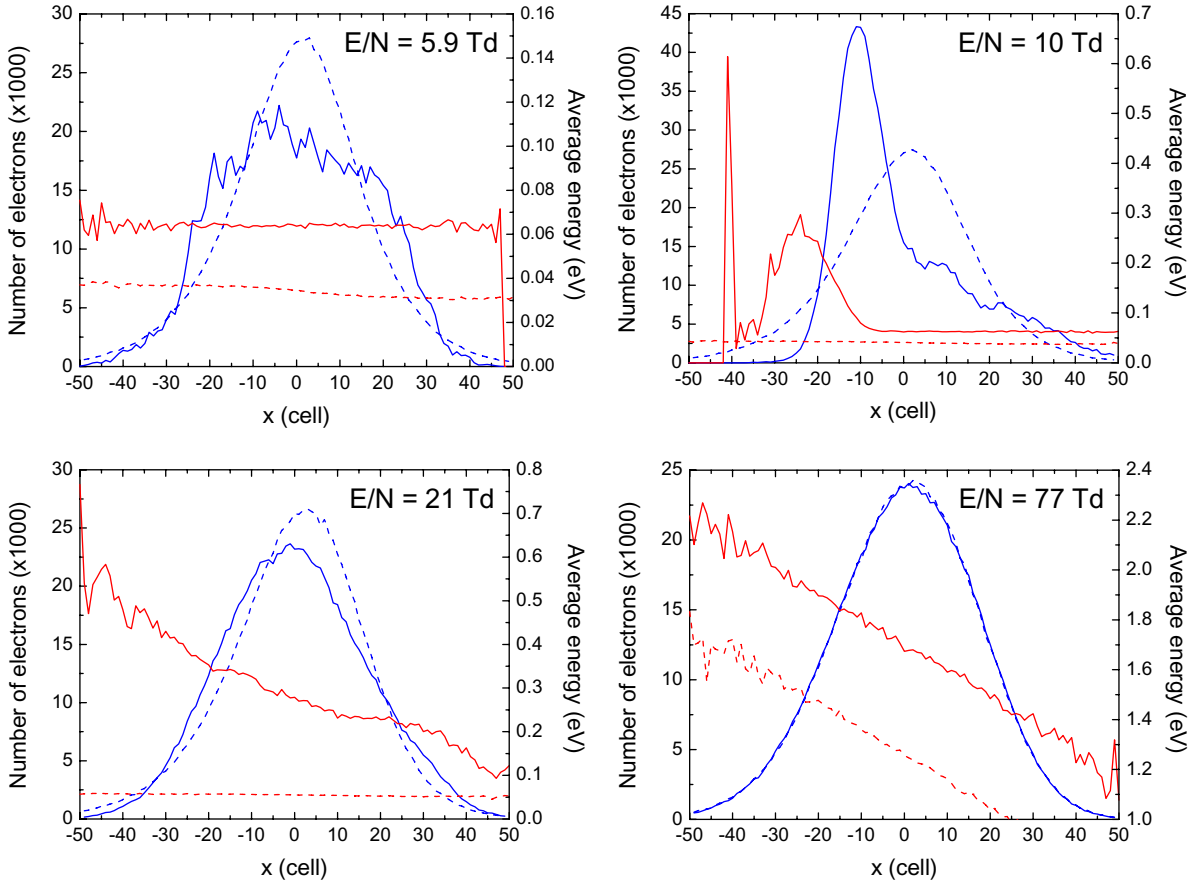


**Figure 8.** Spatial profile of electrons (blue curves) and spatially resolved averaged energy (red curves) at four different *E*/*N* in ALICE timing RPC. Full lines denote the results when electron attachment is treated as a non-conservative process, while the dashed lines represent our results when electron attachment is treated as a conservative inelastic process. ($t$ = 1 ns).

essentially constant otherwise. At the leading edge of the swarm, the average energy is raised with a much steeper slope towards the front. Before reaching the highest energy at the leading edge of the swarm, there is a spatial region where the average energy is first drastically decreased, and then rapidly increased in a very narrow spatial region. For *E*/*N* = 21 Td the spatial dependence of the average energy is almost linear and no sharp jumps and drop-offs in the profile are observed. For increasing *E*/*N* the average electron energy increases and there are fewer and fewer electrons available for attachment. Thus the explicit contribution of electron attachment is further reduced which in turns removes the differences between the bulk and flux components of the drift velocity and diffusion coefficients in the energy region where NDC occurs. Finally for *E*/*N* = 77 Td, the spatial profile of electrons almost coincides with the profile obtained under conditions when electron attachment is treated as a conservative inelastic process. In both cases the average energy linearly increases from the trailing edge towards the leading part of the swarm. This is regime when electron attachment has no longer dominant control over the electron swarm behavior.

The spatially resolved attachment rates are shown in figure 9 and are calculated under the same conditions as for the spatial profile of the electrons and spatially averaged energy. They have complex profiles that reflect the overlap of the average energy and the corresponding cross sections. The

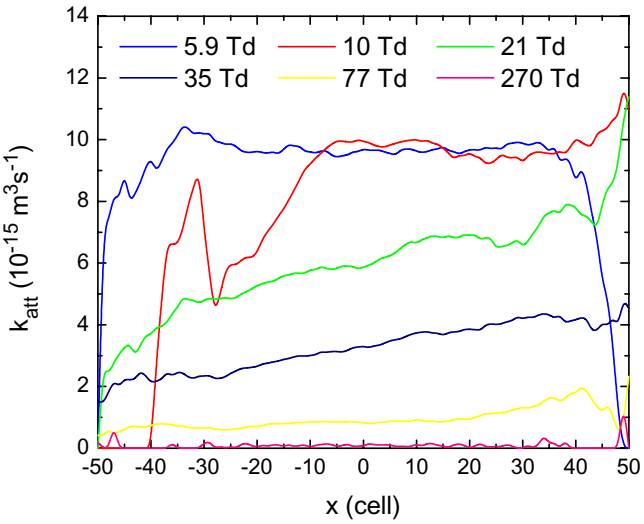


**Figure 9.** Spatially resolved attachment rate coefficient for a range of *E*/*N* in ALICE timing RPC. ($t$ = 1 ns).

attachment rate is generally higher at the trailing edge of the swarm where the average energy of the electrons is lower and exactly these lower energy electrons are most likely to be consumed by electron attachment. This results in a forward shift of the centre of mass of the electron swarm, which is observable as an increase of the bulk drift velocity over the flux

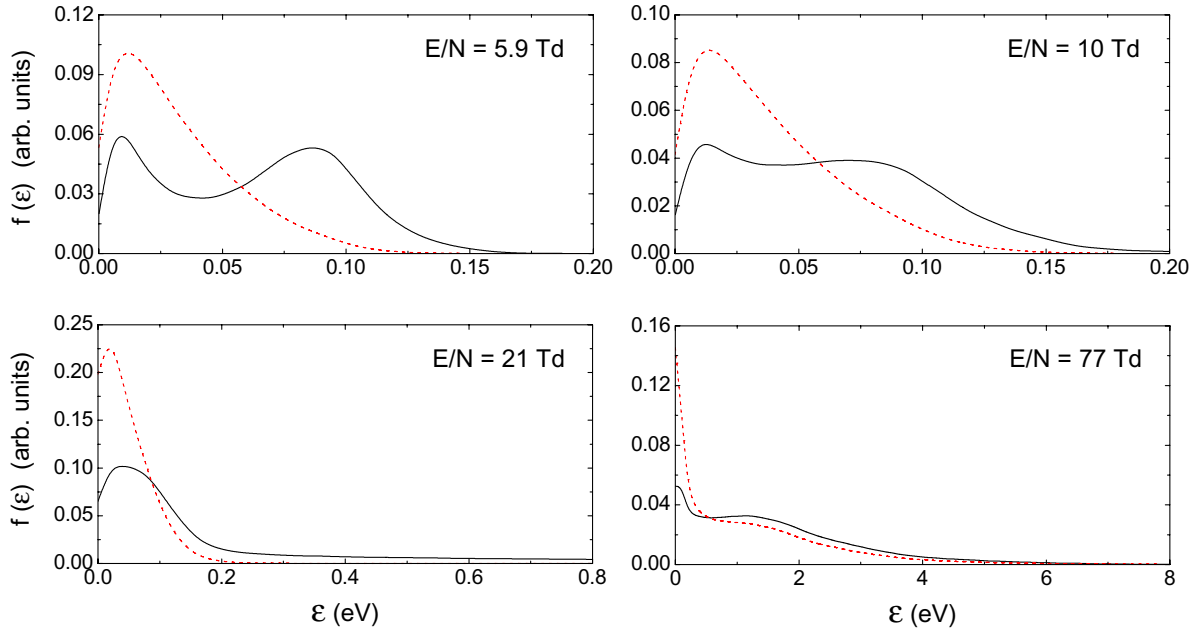


**Figure 10.** Electron energy distribution functions for four different *E*/*N* in ALICE timing RPC. Black lines denote the results when electron attachment is treated as non-conservative process while dashed red lines represent our results when electron attachment is treated as a conservative inelastic process. ($t$ = 1 ns).

values as discussed above. For increasing *E*/*N* the spatially resolved rate coefficients are decreased suggesting much less impact of electron attachment on the electron swarm behavior.

When electron transport is greatly affected by non-conservative collisions it is often very useful to look at the energy distribution functions in order to make conclusions about the underlying physics of some processes. In figure 10 we show the electron energy distribution functions for the same four values of *E*/*N* considered above. The electron energy distribution functions are calculated when electron attachment is treated regularly as a true non-conservative process (black line) and under conditions when electron attachment is assumed to be a conservative inelastic process (dash red line). We see that strong electron attachment induces a 'hole burning' in the electron energy distribution function. For decreasing *E*/*N* the electron energy is generally reduced and the attachment cross section becomes larger. As a result the effect of electron loss on the distribution function increases. This phenomenon has been extensively discussed for electrons in $O_2$ [52] and $O_2$ mixtures [29, 53] and under conditions leading to the phenomenon of absolute negative electron mobility [26, 27]. The same effect is not present when attachment is treated as a conservative inelastic process. Under these conditions, we see that the population of low energy electrons is much higher than the corresponding situation when electron attachment is treated regularly. For increasing *E*/*N*, the population of high energy electrons becomes well described even when electron attachment is treated as a conservative inelastic process.

## 4. Conclusion

In this work, we have presented the results of a systematic investigation of non-conservative electron transport in the mixtures of $C_2H_2F_4$, iso-$C_4H_{10}$ and $SF_6$ used in RPCs in ALICE, CMS and ATLAS experiments at CERN. We have considered conditions consistent with the electrons in an avalanche and streamer mode of operation of these RPC systems with partial motivation being the provision of transport coefficients to be employed in fluid modeling of such systems. Transport coefficients presented in this work are given as a function of *E*/*N* and are accurate to within 2% . The *E*/*N*-dependence of electron transport coefficients for ALICE triggering, CMS and ATLAS RPC systems are almost identical due to similar composition of the corresponding gas mixtures. The bulk drift velocity is slightly higher than flux component even for lower *E*/*N* indicating the presence of attachment heating. When ionization dominates attachment the difference between the bulk and flux drift velocities is further increased. The most striking phenomenon observed in this work is the existence of NDC in the bulk drift velocity component with no indication of any NDC for the flux component in the ALICE timing RPC system. This phenomenon was predicted as possible [48] but has never been observed for electrons primarily as the dominance of explicit effects and strongly energy dependent attachment were sought due to limitations of the momentum transfer theory that was employed in that paper. In order to understand the physical mechanisms behind of this atypical manifestation of the drift velocity, we have calculated spatially resolved transport properties and energy distribution functions for electric fields critical for occurrence of this phenomenon. It was found that the attachment heating governs the phenomenon and plays the dominant role in consideration of non-conservative effects on various transport properties. A 'hole burning' in the distribution function has been observed illustrating the richness and complexity of electron transport phenomena in RPCs.

## Acknowledgments

DB, ZLjP and SD acknowledge support from MPNTRRS Projects OI171037 and III41011. RDW is supported by the Australian Research Council.

## References

[1] Santonico R and Cardarelli R 1981 *Nucl. Instrum. Methods* **187** 377–80
[2] Riegler W, Lippmann C and Veenhof R 2003 *Nucl. Instrum. Methods* A **500** 144–62
[3] Riegler W and Lippmann C 2004 *Nucl. Instrum. Methods* A **518** 86–90
[4] Santonico R 2012 *Nucl. Instrum. Methods* A **661** S2–5
[5] Fonte P 2002 *IEEE Trans. Nucl. Sci.* **49** 881–7
[6] Fonte P 2013 *J. Instrum.* **8** P11001
[7] The ATLAS Collaboration 2008 *J. Instrum.* **3** S08003
[8] The ALICE Collaboration 2008 *J. Instrum.* **3** S08002
[9] The CMS Collaboration 2008 *J. Instrum.* **3** S08004
[10] Blanco A, Couceiro M, Crespo P, Ferreira N C, Ferreira Marques R, Fonte P, Lopes L and Neves J A 2009 *Nucl. Instrum. Methods* A **602** 780–3
[11] Couceiro M, Crespo P, Mendes L, Ferreira N, Ferreira Marques R and Fonte P 2012 *Nucl. Instrum. Methods* A **661** S156–8
[12] Cârloganu C *et al* 2013 *Geosci. Instrum. Methods Data Syst.* **2** 55–60
[13] Abbrescia M, Cassano V, Nuzzo S, Piscitelli G, Vadruccio D and Zaza S 2012 *Nucl. Instrum. Methods* A **661** S190–3
[14] Riegler W 2009 *Nucl. Instrum. Methods* A **602** 377–90
[15] Mangiarotti A, Fonte P and Gobbi A 2004 *Nucl. Instrum. Methods* A **533** 16–21
[16] Khosravi Khorashad L, Moshaii A and Hosseini S 2011 *Europhys. Lett.* **96** 45002
[17] Khosravi Khorashad L, Eskandari M and Moshaii A 2011 *Nucl. Instrum. Methods* A **628** 470–3
[18] Moshaii A, Khosravi Khorashad L, Eskandari M and Hosseini S 2012 *Nucl. Instrum. Methods* A **661** S168–71
[19] Petrović Z Lj, Dujko S, Marić D, Malović G, Nikitović Ž, Šašić O, Jovanović J, Stojanović V and Radmilović-Rađenović M 2009 *J. Phys. D: Appl. Phys.* **42** 194002
[20] White R D, Robson R E, Dujko S, Nicoletopoulos P and Li B 2009 *J. Phys. D: Appl. Phys.* **42** 194001
[21] Biagi S F 1999 *Nucl. Instrum. Methods* A **421** 234–40
[22] Doroud K, Afarideh H, Hatzifotiadou D, Rahighi J, Williams M C S and Zichichi A 2009 *Nucl. Instrum. Methods* A **610** 649–53
[23] Robson R E 1991 *Aust. J. Phys.* **44** 685
[24] Lopes L, Fonte P and Mangiarotti A 2012 *Nucl. Instrum. Methods* A **661** S194–7
[25] Christophorou L G and Olthoff J K 2000 *J. Phys. Chem. Ref. Data* **29** 267
[26] Dyatko N A, Napartovich A P, Sakadzic S, Petrovic Z and Raspopovic Z 2000 *J. Phys. D: Appl. Phys.* **33** 375–80
[27] Dujko S, Raspopovic Z M, Petrovic Z L and Makabe T 2003 *IEEE Trans. Plasma Sci.* **31** 711–6
[28] Bošnjaković D, Petrović Z Lj and Dujko S 2014 A microscopic Monte Carlo approach in modeling of resistive plate chambers *J. Instrum.* submitted
[29] Dujko S, Ebert U, White R D and Petrović Z Lj 2011 *Japan. J. Appl. Phys.* **50** 08JC01
[30] Boltzmann L 1872 *Wien. Ber.* **66** 275
[31] Wang-Chang C S, Uhlenbeck G E and de Boer J 1964 *Studies in Statistical Mechanics* **2** (New York: Wiley) p 241
[32] Robson R E and Ness K F 1986 *Phys. Rev.* A **33** 2068–77
[33] Ness K F and Robson R E 1986 *Phys. Rev.* A **34** 2185–209
[34] Dujko S, White R D, Petrović Z Lj and Robson R E 2010 *Phys. Rev.* E **81** 046403
[35] Legler W 1961 *Z. Naturf.* **16a** 253
[36] Raspopović Z M, Sakadžić S, Bzenić S A and Petrović Z Lj 1999 *IEEE Trans. Plasma Sci.* **27** 1241–8
[37] Petrović Z Lj, Raspopović Z M, Dujko S and Makabe T 2002 *Appl. Surf. Sci.* **192** 1–25
[38] Li Y M, Pitchford L C and Moratz T J 1989 *Appl. Phys. Lett.* **54** 1403
[39] Yousfi M, Hennad A and Alkaa A 1994 *Phys. Rev.* E **49** 3264–73
[40] Dujko S, Markosyan A H, White R D and Ebert U 2013 *J. Phys. D: Appl. Phys.* **46** 475202
[41] Markosyan A H, Dujko S and Ebert U 2013 *J. Phys. D: Appl. Phys.* **46** 475203
[42] Šašić O, Dupljanin S, de Urquijo J and Petrović Z Lj 2013 *J. Phys. D: Appl. Phys.* **46** 325201
[43] Itoh H, Matsumura T, Satoh K, Date H, Nakao Y and Tagashira H 1993 *J. Phys. D: Appl. Phys.* **26** 1975–9
[44] Bošnjaković D, Dujko S, Petrović Z Lj 2012 Electron transport coefficients in gases for resistive plate chambers *Proc. of the 26th Summer School and Int. Symp. on the Physics of Ionized Gases* (Zrenjanin, Serbia, 27–31 August) Kuraica M and Mijatović Z (Bristol: IOP) pp 265–8
[45] Bošnjaković D, Petrović Z Lj and Dujko S 2013 Monte Carlo modelling of resistive plate chambers *Proc. of the XVII Int. Workshop on Low-Energy Positron and Positronium Physics and the XVIII Int. Symposium on Electron-Molecule Collisions and Swarms* (Kanazawa, Japan, 19–21 July) p 44
[46] Petrović Z Lj, Crompton R W and Haddad G N 1984 *Aust. J. Phys.* **37** 23
[47] Robson R E 1984 *Aust. J. Phys.* **37** 35
[48] Vrhovac S B and Petrović Z Lj 1996 *Phys. Rev.* E **53** 4012–25
[49] Banković A, Dujko S, White R D, Marler J P, Buckman S J, Marjanović S, Malović G, García G and Petrović Z Lj 2012 *New J. Phys.* **14** 035003
[50] Banković A, Dujko S, White R D, Buckman S J and Petrović Z Lj 2012 *Nucl. Instrum. Methods* B **279** 92–5
[51] Dujko S, White R D, Raspopović Z M and Petrović Z Lj 2012 *Nucl. Instrum. Methods* B **279** 84–91
[52] Skullerud H R 1983 *Aust. J. Phys.* **36** 845
[53] Hegerberg R and Crompton R W 1983 *Aust. J. Phys.* **36** 831

PUBLISHED BY IOP PUBLISHING FOR SISSA MEDIALAB

RECEIVED: *May 26, 2014*
ACCEPTED: *August 13, 2014*
PUBLISHED: *September 22, 2014*

# A microscopic Monte Carlo approach to modeling of Resistive Plate Chambers

**D. Bošnjaković,**[a,b,1] **Z.Lj. Petrović**[a,b] **and S. Dujko**[a]

[a] *Institute of Physics,*
*University of Belgrade, Pregrevica 118, 11070 Belgrade, Serbia*
[b] *Faculty of Electrical Engineering,*
*University of Belgrade, Bulevar kralja Aleksandra 73, 11120 Belgrade, Serbia*

*E-mail:* dbosnjak@ipb.ac.rs

ABSTRACT: We present a "microscopic" approach in modeling of Resistive Plate Chambers where individual electrons and their collisions with the gas molecules are followed using a Monte Carlo simulation technique. Timing resolutions and efficiencies are calculated for a specific timing RPC with 0.3 mm gas gap and gas mixture of 85% $C_2H_2F_4$ + 5% iso-$C_4H_{10}$ + 10% $SF_6$. Calculations are performed for different sets of cross sections for electron scattering in $C_2H_2F_4$ and primary cluster size distributions. Results of calculations are compared with those obtained in experimental measurements. Electron avalanche fluctuations are also studied and compared with analytical models.

KEYWORDS: Resistive-plate chambers; Detector modelling and simulations II (electric fields, charge transport, multiplication and induction, pulse formation, electron emission, etc); Charge transport and multiplication in gas; Gaseous detectors

[1] Corresponding author.



doi:10.1088/1748-0221/9/09/P09012

2014 JINST 9 P09012

## Contents



## 1 Introduction

Developed in the 1980s [1, 2], Resistive Plate Chambers (RPCs) became widely used particle detectors in high energy physics experiments [3–5]. Electrodes of highly resistive material, such as glass or bakelite, make them free from destructive discharges. They also show remarkable timing resolutions of about 50 ps [6]. Due to their simple construction and low cost, they are often used for large area timing and triggering purposes, but other applications such as medical imaging were also considered [7].

Despite their apparent simplicity, modeling of RPCs is not an easy task because of various physical phenomena ranging from charge generation, transport and multiplication, to signal induction, propagation and electrode relaxation effects, all occurring on different time scales. Yet, many RPC models were developed and published [8]. Most numerical models are based on either the Monte Carlo simulation technique [9, 10] or on the fluid equations [11, 12]. The latter can only provide the mean values of RPC signals in a deterministic fashion while the Monte Carlo models usually follow some theoretical distributions for primary ionization and electron avalanche fluctuations in order to calculate the RPC performance characteristics such as timing resolution, efficiency and charge spectrum. On the other hand, while often being approximate, only the analytical models [13, 14] can provide general conclusions about the influence of different parameters on the RPC performance. These models can also include the stochastic effects in physics of RPCs.

Every RPC model relies on accurate data for electron swarm transport in gases. These parameters include the transport coefficients (e.g. drift velocity and diffusion coefficients) and rate coefficients (e.g. attachment and ionization rate) which are usually calculated from electron impact cross sections using a computer code based on either Monte Carlo method or Boltzmann equation



2014 JINST 9 P09012

analysis. A Monte Carlo code that is often used for such purpose — MAGBOLTZ 2 [15, 16] has cross sections imbedded into the code. Thus cross sections cannot be easily modified, compared or presented. The questions associated with the reliability of cross sections for electron scattering in RPC's gases were already raised in case of $C_2H_2F_4$ [17], which is the main component in gas mixtures for RPCs operated in avalanche mode. As will be shown, the final results that describe the RPC performance may differ considerably depending on the cross sections used.

In this paper, we follow a completely different approach in RPC modeling. Our approach is based on 3D tracking of individual electrons and their collisions with the background gas in a typical Monte Carlo fashion. Here the avalanche fluctuations and the RPC performance characteristics emerge naturally from the stochastic character of electron collisions and are determined exclusively by the cross sections for electron scattering. Such an approach based on MAGBOLTZ was used for the calculation of gas gain fluctuations [18] but still, no such attempts in RPC modeling were published [17].

This paper is organized as follows. First, we discuss our simulation technique (section 2). Then, we present the results for electron avalanches in an infinite space (sections 3.2 and 3.3) which are used for comparison with the analytical models of avalanche development and timing. Finally, the boundaries are introduced (section 3.4) and timing and efficiency are calculated for a specific timing RPC (0.3 mm gas gap, gas mixture of 85% $C_2H_2F_4$ + 5% iso-$C_4H_{10}$ + 10% $SF_6$). A study is made with different cross section sets and cluster size distributions. The results are compared with experimental values. Due to limited computing resources we are only able to use a relatively low value of signal threshold of about $10^6$ electrons which excludes the space charge effects.

## 2 Simulation technique

Our simulation technique for an RPC event (i.e. passage of an incoming particle) can be divided into a few steps. First, we generate the primary ionization, e.g., the initial electrons due to passage of the incoming particle. The individual electrons and their collisions with the background gas are then traced between the moments of sampling. In these moments, we record some quantities (e.g. number of electrons) and calculate the induced signal. Sampling interval is set to 0.2 ps. The threshold crossing time is determined using the exponential interpolation between the samples. The simulation consisting of 10000 events usually takes approximately two days of computation time on a multiprocessor system with about 300 active CPU cores @ 2.1 GHz.

### 2.1 Primary ionization

Primary ionization is generated according to a commonly used model. The primary electrons are grouped in clusters. Electrons belonging to the same cluster have the same initial position. Number of electrons in the cluster is generated using a cluster size distribution. The positions of the clusters are generated using exponential distribution for the distance between neighboring clusters

$$P(x) = \frac{1}{\lambda} \exp\left(-\frac{x}{\lambda}\right),$$

where $\lambda$ is the mean distance between clusters. Initial velocity of primary electrons is chosen according to the Maxwellian velocity distribution with the mean electron energy of 1 eV. Mean



2014 JINST 9 P09012

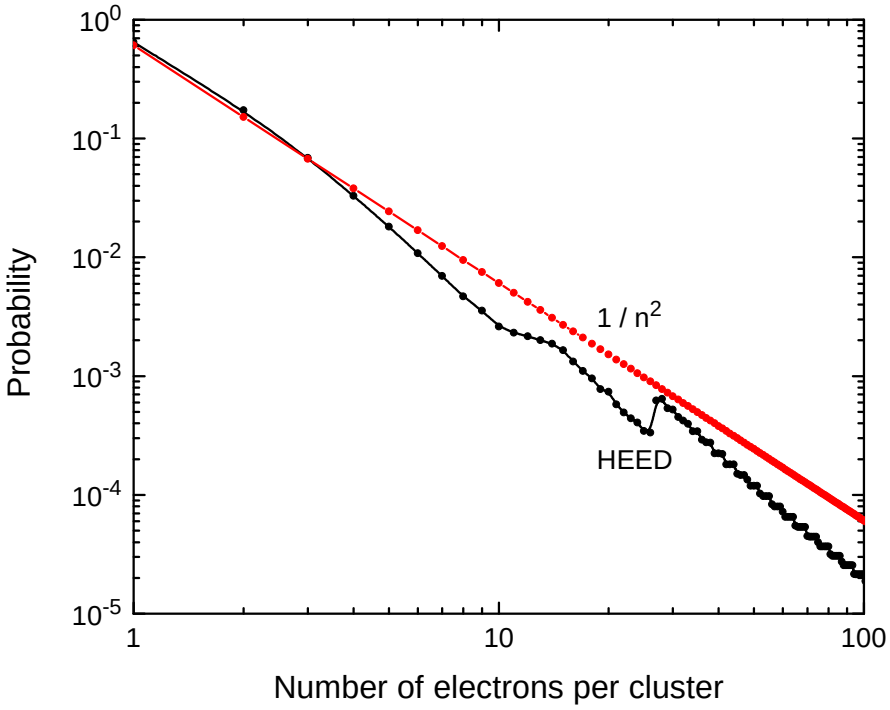


**Figure 1**. Cluster size distribution calculated by HEED, and $1/n^2$ model.

distance between the clusters and cluster size distribution are calculated using a computer program HEED [19, 20]. For minimum ionizing particles, we have obtained a value of 8.44 clusters/mm, which differs from 7.5 clusters/mm quoted in [21]. Considering the arguments and measurements presented in [21], we have decided to use the value of 7.5 clusters/mm since it seems more realistic. For cluster size distributions we use two models in our simulations for comparison: the $1/n^2$ model and the distribution calculated by HEED (figure 1). Both distributions are cut to 500 electrons.

### 2.2 Electron tracking

In the work reported here, the Monte Carlo method is used to simulate the motion of electrons in the background gas. In the present Monte Carlo code both elastic and inelastic collisions are assumed to occur in the interactions of the electrons with the gas molecules. The electron-electron interactions are neglected since the transport is considered in the limit of low electron density. Calculations are performed at zero gas temperature and isotropic scattering is assumed to occur in all electron-molecule collisions regardless of the nature of specific processes or energy.

Spatiotemporal evolution of each electron is followed through a time step determined from the mean free time between collisions. This small time step is used to solve the integral equation for the collision probability in order to determine the time of the next collision. This can be done using either the null collision technique or integration technique. In our code (and in contrast to MAGBOLTZ) the latter approach is employed. The number of time steps is determined in such a way as to optimize the performance of the Monte Carlo code without reducing the accuracy of the final results. After a collision has occurred, it is then determined whether the electron has collided elastically or experienced one of the several possible types of inelastic events, by using the relative



2014 JINST 9 P09012

probabilities of various collision types. When an elastic collision has occurred, the electron energy is reduced by the amount $2m/M$ where $m$ and $M$ are the electron and molecule masses, respectively. In an inelastic collision the electron is assumed to lose an amount of energy corresponding to the energy loss for that particular process. After ionization, it is assumed that all fractions of the distribution of the available energy are equally probable between primary and secondary electrons. When electron attachment takes place, the consumed electron is simply removed from the simulation. Under the hypothesis of isotropic scattering, the change in direction of the electron velocity after a collision is expressed by uniformly distributed scattering angle within interval $[0,\pi]$ and by the azimuthal angle uniformly distributed within the interval $[0,2\pi]$. For more details on our Monte Carlo simulation technique the reader is referred to our recent reviews [22–24].

In the present work we have employed three different sets of cross sections for electron scattering in $C_2H_2F_4$: 1) a set recently developed by our group [25], 2) a set from MAGBOLTZ 2.8.9 (2010), and 3) a set from MAGBOLTZ 2.7.1 (pre-2010). The set developed by our group and the set from MAGBOLTZ 2.8.9 have been recently updated and modified on the basis of new experimental measurements of electron transport data in $C_2H_2F_4$ under the pulsed Townsend conditions [26]. For electron scattering in iso-$C_4H_{10}$, we have used a set of cross sections from MAGBOLTZ 2.7.1. There is an updated version of the same cross sections hard-coded in more recent versions of MAGBOLTZ but our calculations have revealed much better agreement between our data for ionization coefficient and those experimentally measured [27], if the cross sections from MAGBOLTZ 2.7.1 are considered [27, 28]. Finally, for electron scattering in $SF_6$ we have employed a set of cross sections developed by Itoh et al. [29].

### 2.3 Signal induction

The induced current in an electrode is calculated using Ramo's theorem [30]:

$$i(t) = \frac{E_w}{V_w} \cdot q \cdot n(t) \cdot w(t)\,,$$

where $E_w$ is the weighting field of the electrode (calculated as electric field in the gas gap when the electrode is raised to the potential of $V_w$ while the other electrodes are grounded), $q$ is the electron charge, and $n$ is the number of electrons and $w$ represents the flux drift velocity. The flux drift velocity is the average electron velocity while the bulk drift velocity is defined as velocity of center of mass of the electron swarm (avalanche) [31, 32]. The two may differ quantitatively and sometimes even qualitatively when non-conservative collisions such as attachment and/or ionization are present [33]. For our RPC geometry (0.3 mm gas gap, one metallic and one 3 mm thick glass electrode with $\epsilon_r = 8$) the weighting field of 1.48/mm was calculated. The induced charge is calculated as an integral of the induced current, $q(t) = \int_0^t i(\tau)\,d\tau$.

## 3 Results and discussion

### 3.1 Preliminaries

First we give a brief summary of the most important parameters used in the following sections. We consider the gas mixture of 85% $C_2H_2F_4$, 5% iso-$C_4H_{10}$ and 10% $SF_6$ and the gas number density is set to $N = 2.505 \cdot 10^{25}$ m$^{-3}$ which corresponds to the pressure of 1 atm and temperature of 20 °C).



2014 JINST 9 P09012

**Table 1**. Calculated $S = (\alpha - \eta)w$ and $k = \eta/\alpha$ parameters for a mixture of 85% $C_2H_2F_4$ + 5% iso-$C_4H_{10}$ + 10% $SF_6$ with three different $C_2H_2F_4$ cross section sets. All calculations presented here are made using our Monte Carlo method.

| E/N | *Our set* | | *MAGBOLTZ 2.8.9 set* | | *MAGBOLTZ 2.7.1 set* | |
|---|---|---|---|---|---|---|
| *(Td)* | S ($10^{10}$ $s^{-1}$) | k | S ($10^{10}$ $s^{-1}$) | k | S ($10^{10}$ $s^{-1}$) | *k* |
| 359 | $1.27 \pm 0.04$ | $0.20 \pm 0.01$ | $1.40 \pm 0.04$ | $0.16 \pm 0.01$ | $1.66 \pm 0.04$ | $0.16 \pm 0.01$ |
| 385 | $1.62 \pm 0.04$ | $0.16 \pm 0.01$ | $1.77 \pm 0.04$ | $0.13 \pm 0.01$ | $2.14 \pm 0.04$ | $0.13 \pm 0.01$ |
| 412 | $2.01 \pm 0.04$ | $0.13 \pm 0.01$ | $2.20 \pm 0.04$ | $0.10 \pm 0.01$ | $2.68 \pm 0.05$ | $0.10 \pm 0.01$ |
| 439 | $2.43 \pm 0.05$ | $0.11 \pm 0.01$ | $2.67 \pm 0.05$ | $0.08 \pm 0.01$ | $3.26 \pm 0.05$ | $0.08 \pm 0.01$ |

The reduced electric field $E/N$ is expressed in Td (1 Td = $10^{-21}$ $Vm^2$). The primary ionization is generated assuming the mean value of 7.5 clusters/mm for minimum ionizing particles. Velocity of the initial electron(s) is chosen according to the Maxwellian velocity distribution with the mean starting energy of 1 eV. Induced signal is calculated using the weighting field of $E_w/V_w = 1.48/\text{mm}$. The gas gap is 0.3 mm.

Our simulation results are compared with those obtained in an analytical model for time response functions [13]. The model shows that, except for small thresholds (e.g. less than 1000 electrons), the RPC time response function can be written as

$$\rho(n_{\text{th}},t) = \frac{1}{2\pi i}\oint_{|z|=r} \frac{\exp(n_{\text{cl}}F(z))-1}{\exp(n_{\text{cl}})-\exp(n_{\text{cl}}F(1/k))}\frac{(1-k^2)n_{\text{th}}S}{(1-kz)^2}\cdot \\ \cdot\exp\left(-St - n_{\text{th}}\frac{(1-k)(1-z)}{1-kz}\exp(-St)\right)dz, \tag{3.1}$$

where $n_{\text{th}}$ and $n_{\text{cl}}$ are the threshold given as number of electrons and the mean number of clusters (in our simulation $2.25 = 7.5/\text{mm} \cdot 0.3$ mm gas gap), respectively; $F(z)$ and $S = (\alpha - \eta)w$ are the $Z$-transform of cluster size distribution with radius of convergence $r_F$ and the effective ionization rate, respectively; $\alpha$ and $\eta$ are the ionization coefficient and attachment coefficient, respectively; and $w$ is the flux drift velocity and $k = \eta/\alpha$. The integration is made over a circle with radius $r_F < r < 1/k$. Using the expression (3.1), it can easily be shown that the shape of the time response function does not depend on the threshold level. It is only shifted in time, and thus the timing resolution does not depend on the threshold. This is a well know experimental observation [6]. One should note that this model does not include the space charge effects and the effects induced by the gas gap boundaries, i.e. an infinite space is assumed. In addition, when comparison is made with our timing distributions, the theoretical time response functions (3.1) are shifted in time so that their mean threshold crossing time is equal to that of simulated data. Table 1 shows the $S$ and $k$ parameters for different $C_2H_2F_4$ cross section sets and electric field strengths calculated using our Monte Carlo method described in section 2.2.

The analytical model presented above is based on the Legler's basic theory of avalanche statistics [34]. This theory is also used by some other analytical and numerical models [8]. According to this theory the probability for an avalanche, initiated by one electron, to have $n$ electrons after



2014 JINST 9 P09012

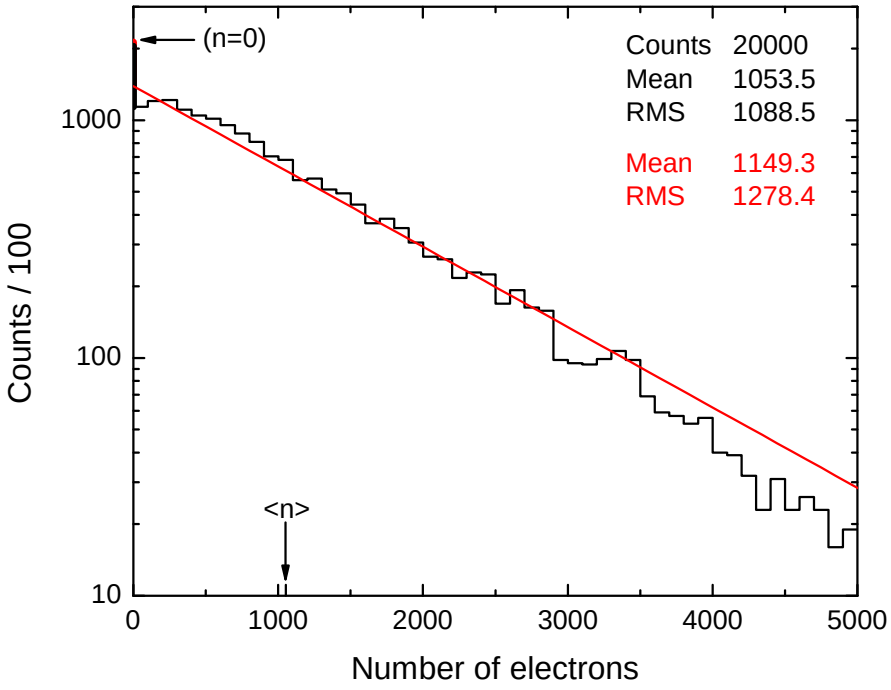


**Figure 2**. Avalanche size distribution at $t = 290$ ps. (Red) comparison with Legler's model (3.2). Our cross sections for $C_2H_2F_4$ [25] are assumed. $E/N = 439$ Td.

path $x$ is given by

$$P(n,x) = \begin{cases} k\,\dfrac{\bar{n}(x)-1}{\bar{n}(x)-k}, & n=0 \\ \bar{n}(x)\left(\dfrac{1-k}{\bar{n}(x)-k}\right)^2\left(\dfrac{\bar{n}(x)-1}{\bar{n}(x)-k}\right)^{n-1}, & n>0 \end{cases} \tag{3.2}$$

where $\bar{n}(x) = \exp((\alpha-\eta)x)$ is the mean avalanche size at the position $x$. This distribution has a characteristic exponential shape which has been experimentally confirmed for many gases at lower electric field strengths. But at higher electric fields, a prominent deviation was noticed and could be attributed to the approximation of constant ionization coefficient used by this model [35]. Also, one should bear in mind that $x$ is the position of avalanche center of mass and therefore $\alpha$ and $\eta$ should be regarded as "bulk" coefficients, i.e. calculated using the bulk drift velocity. However, if the probability $P(n,x)$ is considered as time dependent (3.1), then the distinction between flux and bulk values is not necessary since in each case $\bar{n}$ reduces to $\bar{n}(t) = \exp(St)$ where $S$ is the effective ionization rate.

### 3.2 Single-electron avalanches

First we present the results of simulation for 20000 avalanches in an infinite space initiated by a single electron. The results for the avalanche size distribution (figure 2) are useful for comparison with Legler's theory of avalanche statistics which is often used in many RPC simulations and modeling [8]. Results show a deviation from the predicted exponential dependence (3.2) mostly prominent at small avalanche sizes. This deviation follows from an approximation of constant first



2014 JINST 9 P09012

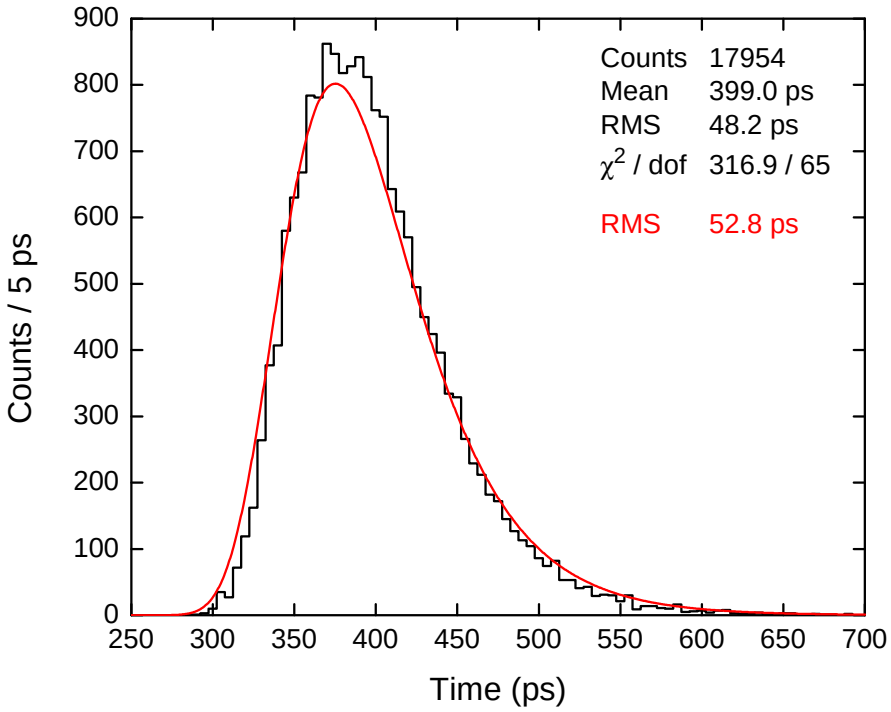


**Figure 3**. Timing distribution for single electron avalanches. The threshold is set to 10000 electrons and our cross sections for $C_2H_2F_4$ [25] are assumed. $E/N = 439$ Td.

Townsend ionization coefficient, assumed by Legler's basic model. In reality, however, the ionization coefficient varies during avalanche development, especially in the initial stages where only one or just a few electrons are present. Without going into further details, it should be mentioned that there have been several attempts to describe and to deal with this issue in Legler's theory [36]. Unfortunately, even after setting aside the question of their validity and justification, each of these attempts makes the solution for the avalanche size distribution unobtainable in closed form. On the other hand, microscopic Monte Carlo approach does not have to deal with these approximations since the avalanche statistics arise naturally from the stochastic character of electron-molecule collisions. This is the key difference between our model and the other RPC models based on theoretical avalanche size distributions (mostly Legler or Polya type).

Figure 3 shows the timing distribution for a threshold of 10000 electrons. The expected theoretical distribution was calculated using the time response function for the case of single electron avalanches [13]:

$$\rho(n_{\mathrm{th}},t) = \frac{n_{\mathrm{th}} S(1-k)}{1-\exp(-n_{\mathrm{th}}(1-k))} \exp\left(-St - n_{\mathrm{th}}(1-k)\exp(-St)\right) .$$

The slight disagreement with the theoretical distribution can be attributed to the same cause as the disagreement between avalanche size distributions discussed in the previous paragraph. Since the corresponding theoretical avalanche size distribution is "wider" (i.e. has larger standard deviation) than the simulated one, we expected the same for the timing distribution, which is the case. A test was also made with different energy distribution for the initial electron as in the late stage of avalanche development (mean energy of 6.7 eV). The test showed that the higher initial electron en-



2014 JINST 9 P09012

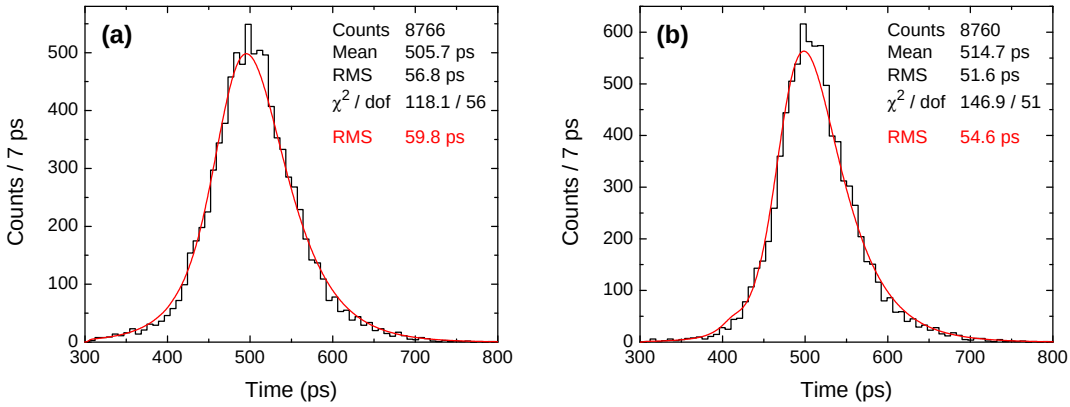


**Figure 4**. Timing distribution for avalanches started by primary ionization generated using (a) $1/n^2$, (b) HEED cluster size distribution. Infinite space. The threshold is set to $10^6$ electrons and our cross sections for $C_2H_2F_4$ [25] are assumed. $E/N = 439$ Td.

ergy had practically no effect on the r.m.s. value of threshold crossing times (it was lower by 0.2 ps) while the number of avalanches which reached the threshold was slightly higher (18350). The latter was expected since the initial electron with higher energy had a lower probability for attachment.

### 3.3 Avalanches started by primary ionization

The case of avalanches started by primary ionization progressing in an infinite space was also studied. The primary ionization was generated according to the model described in section 2.1. Simulations with 10000 events were made for $1/n^2$ and HEED cluster size distributions. Figure 4 shows the timing distribution for a threshold of $10^6$ electrons. The theoretical distributions were calculated using the model (3.1). Slightly higher theoretical r.m.s. values have already been discussed in the previous section. As of distribution shape, one can see that the left tail of the distribution for the $1/n^2$ case is wider than in the case where HEED cluster size distribution was used. This is expected since the left tail represents the fastest events which most often come from high primary ionization, and the probability for large primary clusters is higher in the case of $1/n^2$ distribution (figure 1). The same reasoning applies for the difference between r.m.s. values for the $1/n^2$ and HEED case.

### 3.4 Full model with primary ionization and boundaries

We now consider the effects of boundaries with gas gap set to 0.3 mm. Avalanches initiated by primary ionization move towards the anode due to electric field. When an electron reaches the anode it is removed from the simulation. Figure 5 shows the results for timing distribution with a threshold of $10^6$ electrons. Since the simulation also consists of 10000 events, comparing the number of events which reached the threshold with the one from the previous case without boundaries, one can see the "absorbing effect" of the anode. Also, a slightly higher r.m.s. value can be attributed to the uncertainty of cluster positions, especially the ones closest to the anode which are the first to be absorbed.

The same simulation was performed for a threshold of 2 fC of induced charge. This value corresponds to about $10^6$ electrons in the gas gap when the threshold is reached. One could expect



2014 JINST 9 P09012

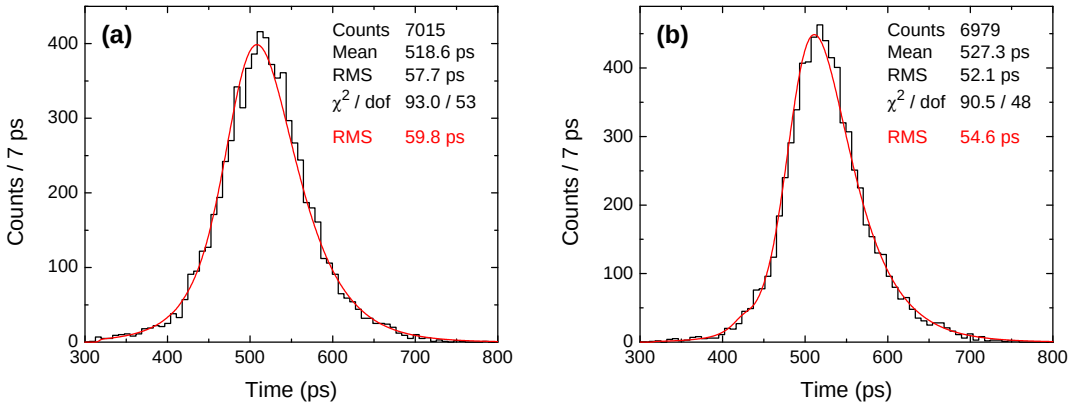


**Figure 5**. Timing distribution for avalanches started by primary ionization generated using (a) $1/n^2$, (b) HEED cluster size distribution. Gas gap 0.3 mm. The threshold is set to $10^6$ electrons and our cross sections for $C_2H_2F_4$ [25] are assumed. $E/N = 439$ Td.

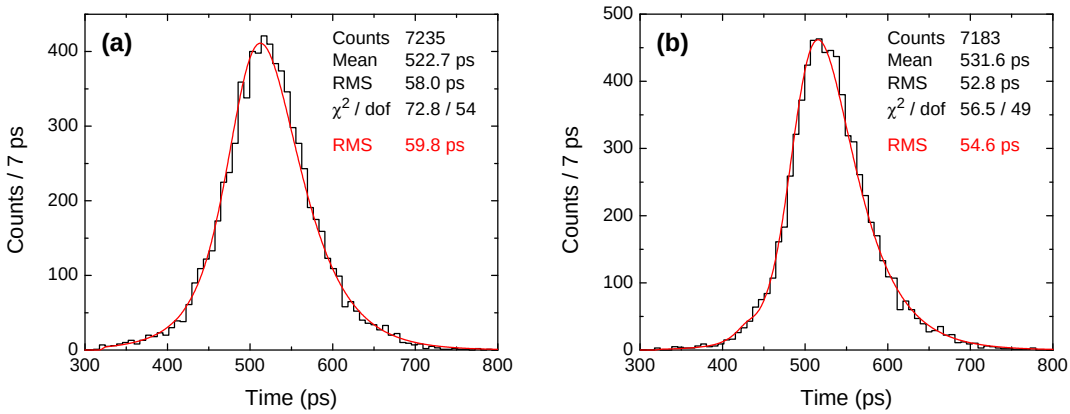


**Figure 6**. Timing distribution for avalanches started by primary ionization generated using (a) $1/n^2$, (b) HEED cluster size distribution. Gas gap 0.3 mm. The threshold is set to 2 fC and our cross sections for $C_2H_2F_4$ [25] are assumed. $E/N = 439$ Td.

somewhat different results when boundaries are present, because this time the threshold is given by induced charge i.e. the integral of the induced current (which is proportional to the number of electrons in the gas gap). However, the results for this case (figure 6) show that practically only the number of events which reached the threshold is slightly higher than in the case when the threshold is $10^6$ electrons. A possible explanation lies in the cumulative character of the induced charge in such way that the avalanches which are absorbed in the anode are not completely "lost" as if they were not present at all. Instead, they contribute to the induced charge, and the other avalanches which would otherwise be too small or too close to the anode to reach the threshold alone, can also contribute so that eventually the threshold is reached.

Finally, we present the results for timing resolution (figure 7) and efficiency (figure 8) of the RPC. The results were made for a range of electric field strengths, different $C_2H_2F_4$ cross section sets and primary cluster size distributions. For each set of parameters 10000 events were simulated with the threshold set to 2 fC. The timing resolution is simply the r.m.s. of the threshold crossing times while the efficiency is the fraction of events which have reached the threshold. Results are



2014 JINST 9 P09012

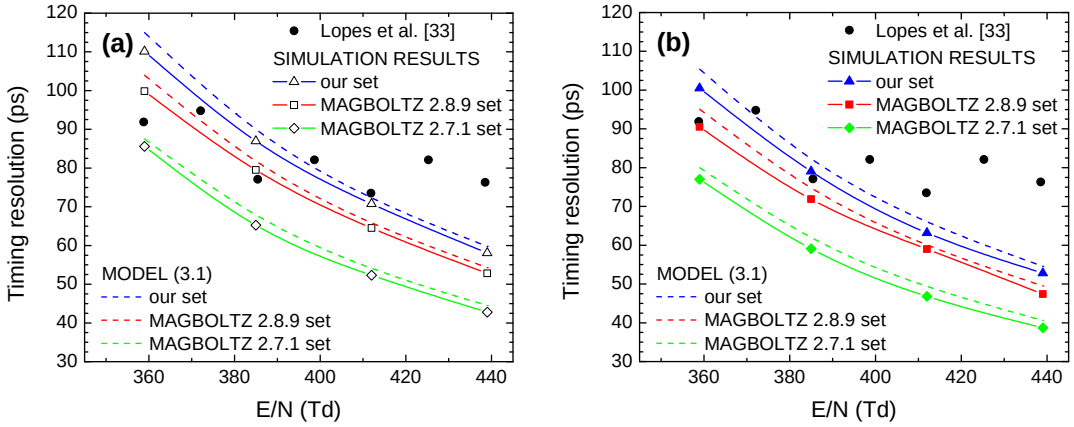


**Figure 7**. Timing resolutions for different $C_2H_2F_4$ cross section sets and primary ionization models, (a) $1/n^2$, (b) HEED cluster size distribution. Comparison with experimental values by Lopes et al. [37].

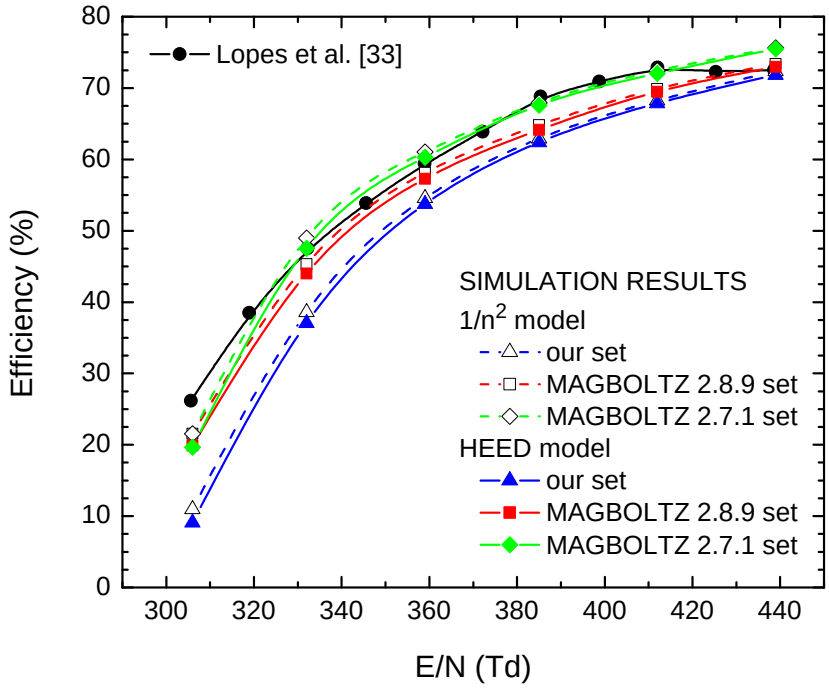


**Figure 8**. Efficiencies for different $C_2H_2F_4$ cross section sets and primary ionization models, (a) $1/n^2$, (b) HEED cluster size distribution. Comparison with experimental values by Lopes et al. [37].

compared with measurements by Lopes et al. [37] which show a clear fluctuation of the timing resolution, probably due to some kind of experimental uncertainty. Also, the measured timing resolutions and efficiencies both show a pronounced saturation effect at higher electric field strengths which is not present in our results. The theoretical timing resolutions, calculated using (3.1), are in good agreement with the simulated ones. The discrepancy between the results for different $C_2H_2F_4$ cross sections sets is expected since the effective ionization rate is the dominant factor in both timing and efficiency [8]. Somewhat higher efficiency in the $1/n^2$ case is a consequence of larger mean cluster size than in the case of HEED cluster size distribution. It should also be mentioned that the



2014 JINST 9 P09012

tests with different energy distributions for the initial electrons showed no effect on the timing, but the efficiencies were higher by 1-2% in case when mean initial electron energy was set to 10 eV.

## 4 Summary and conclusions

A microscopic Monte Carlo approach, based on tracking of individual electrons and their collisions with the gas molecules, was developed and used with the aim of obtaining the performance characteristics of a timing RPC. The development of electron avalanches in infinite space was also studied and the results for threshold crossing times showed good agreement with an analytical model. Since the energy distribution of the initial electrons showed no effect on timing, the minor differences can only be attributed to Legler's basic theory of avalanche statistics, assumed in this analytical model.

The realistic RPC simulations with implemented gas gap boundaries and primary ionization models were performed with three different sets of cross sections for electron scattering in $C_2H_2F_4$. The inclusion of boundaries show no significant effect on timing, unlike the effect of different cross section sets which is very prominent. Overall, the results for timing and efficiency show good agreement with experimental values. Because of limited computing resources, a relatively low value of signal threshold was chosen corresponding to about $10^6$ electrons in the gas gap. Still, the results can be considered valid as the theory and experiments show that the timing resolution does not depend on the threshold level. The extension of the threshold to realistic levels where space charge is present, without sacrifice in accuracy, is an ongoing work.

## Acknowledgments

This work was supported by MPNTRRS Projects OI171037 and III41011.

## References

[1] R. Santonico and R. Cardarelli, *Development of resistive plate counters*, *Nucl. Instrum. Meth.* **187** (1981) 377.

[2] R. Santonico, R. Cardarelli, A. Di Biagio and A. Lucci, *Progress in Resistive Plate Counters*, *Nucl. Instrum. Meth.* **A 263** (1988) 20.

[3] ATLAS collaboration, *The ATLAS experiment at the CERN LHC*, 2008 *JINST* **3** S08003.

[4] ALICE collaboration, *The ALICE experiment at the CERN LHC*, 2008 *JINST* **3** S08002.

[5] CMS collaboration, *The CMS experiment at the CERN LHC*, 2008 *JINST* **3** S08004.

[6] P. Fonte, *Applications and new developments in resistive plate chambers*, *IEEE Trans. Nucl. Sci.* **49** (2002) 881.

[7] G. Georgiev et al., *Multigap RPC for PET: development and optimisation of the detector design*, 2013 *JINST* **8** P01011.

[8] P. Fonte, *Survey of physical modelling in Resistive Plate Chambers*, 2013 *JINST* **8** P11001.

[9] W. Riegler and C. Lippmann, *The physics of resistive plate chambers*, *Nucl. Instrum. Meth.* **A 518** (2004) 86.



2014 JINST 9 P09012

[10] S. Mohammed, R. Hasan, N. Majumdar, S. Mukhopadhyay and B. Satyanarayana, *Simulation studies on the Effect of $SF_6$ in the RPC gas mixture*, PoS(RPC2012)034.

[11] L. Khosravi Khorashad, A. Moshaii and S. Hosseini, *Fast and total charges in a resistive plate chamber: a numerical approach*, *Europhys. Lett.* **96** (2011) 45002.

[12] A. Moshaii, L. Khosravi Khorashad, M. Eskandari and S. Hosseini, *RPC simulation in avalanche and streamer modes using transport equations for electrons andions*, *Nucl. Instrum. Meth.* **A 661** (2012) S168.

[13] W. Riegler, *Time response functions and avalanche fluctuations in resistive plate chambers*, *Nucl. Instrum. Meth.* **A 602** (2009) 377.

[14] A. Mangiarotti, P. Fonte and A. Gobbi, *Exactly solvable model for the time response function of RPCs*, *Nucl. Instrum. Meth.* **A 533** (2004) 16.

[15] S.F. Biagi, *Monte Carlo simulation of electron drift and diffusion in counting gases under the influence of electric and magnetic fields*, *Nucl. Instrum. Meth.* **A 421** (1999) 234.

[16] S. Biagi, *MAGBOLTZ — Program to compute electron transport parameters in gases*, version 2, CERN.

[17] D. Gonzalez-Diaz and A. Sharma, *Current challenges and perspectives in resistive gaseous detectors: a manifesto from RPC 2012*, PoS(RPC2012)084.

[18] H. Schindler, S.F. Biagi and R. Veenhof, *Calculation of gas gain fluctuations in uniform fields*, *Nucl. Instrum. Meth.* **A 624** (2010) 78.

[19] I.B. Smirnov, *Modeling of ionization produced by fast charged particles in gases*, *Nucl. Instrum. Meth.* **A 554** (2005) 474.

[20] I.B. Smirnov, *HEED — Program to compute energy loss of fast particles in gases*, Version 1.01, CERN.

[21] W. Riegler, C. Lippmann and R. Veenhof, *Detector physics and simulation of resistive plate chambers*, *Nucl. Instrum. Meth.* **A 500** (2003) 144.

[22] S. Dujko, Z.M. Raspopović and Z.Lj. Petrović, *Monte Carlo studies of electron transport in crossed electric and magnetic fields in $CF_4$*, *J. Phys.* **D 38** (2005) 2952.

[23] S. Dujko, R.D. White, K.F. Ness, Z.Lj. Petrović and R.E. Robson, *Non-conservative electron transport in $CF_4$ in electric and magnetic fields crossed at arbitrary angles*, *J. Phys.* **D 39** (2006) 4788.

[24] S. Dujko, R.D. White and Z.Lj. Petrović, *Monte Carlo studies of non-conservative electron transport in the steady-state Townsend experiment*, *J. Phys.* **D 41** (2008) 245205.

[25] O. Šašić, S. Dupljanin, J. de Urquijo and Z.Lj. Petrović, *Scattering cross sections for electrons in $C_2H_2F_4$ and its mixtures with Ar from measured transport coefficients*, *J. Phys.* **D 46** (2013) 325201.

[26] J. de Urquijo, A.M. Juárez, E. Basurto and J.L. Hernández-Ávila, *Electron swarm coefficients in 1,1,1,2 tetrafluoroethane (R134a) and its mixtures with Ar*, *Eur. Phys. J.* **D 51** (2009) 241.

[27] I.B. Lima et al., *Experimental investigations on the first Townsend coefficient in pure isobutane*, *Nucl. Instrum. Meth.* **A 670** (2012) 55.

[28] D. Bošnjaković, S. Dujko and Z.Lj. Petrović, *Electron transport coefficients in gases for Resistive Plate Chambers*, in proceedings of the 26th *Summer School and International Symposium on the Physics of Ionized Gases*, August 27, Zrenjanin, Serbia (2012).

2014 JINST 9 P09012

[29] H. Itoh, *Electron transport coefficients in $SF_6$*, *J. Phys.* **D 26** (1993) 1975.

[30] S. Ramo, *Currents induced by electron motion*, *Proc. I.R.E.* **27** (1939) 584.

[31] R.E. Robson, *Transport phenomena in the presence of reactions: definition and measurement of transport coefficients*, *Aust. J. Phys.* **44** (1991) 685.

[32] S. Dujko, R.D. White, Z.M. Raspopović and Z.Lj. Petrović, *Spatially resolved transport data for electrons in gases: definition, interpretation and calculation*, *Nucl. Instrum. Meth.* **B 279** (2012) 84.

[33] S. Dujko, Z.M. Raspopović, Z.Lj. Petrović and T. Makabe, *Negative mobilities of electrons in radio frequency fields*, *IEEE Trans. Plasma Sci. PS* **31** (2003) 711.

[34] W. Legler, *Die Statistik der Elektronenlawinen in elektronegativen Gasen bei hohen Feldstärken und bei grosser Gasverstärkung*, *Z. Naturforsch.* **16a** (1961) 253.

[35] H. Raether, *Electron avalanches and breakdown in gases*, Butterworths, London U.K. (1964).

[36] W. Legler, *The influence of the relaxation of the electron energy distribution on the statistics of electron avalanches*, *Br. J. Appl. Phys.* **18** (1967) 1275.

[37] L. Lopes, P. Fonte and A. Mangiarotti, *Systematic study of gas mixtures for timing RPCs*, *Nucl. Instrum. Meth.* **A 661** (2012) S194.

2014 JINST 9 P09012


# 27th Summer School and International Symposium on the Physics of Ionized Gases

**August 26-29, 2014, Belgrade, Serbia**

# CONTRIBUTED PAPERS

# &

## ABSTRACTS OF INVITED LECTURES, TOPICAL INVITED LECTURES, PROGRESS REPORTS AND WORKSHOP LECTURES

Editors:
Dragana Marić
Aleksandar R. Milosavljević
Zoran Mijatović

Institute of Physics, Belgrade
University of Belgrade


Serbian Academy
of Sciences and Arts

www.spig2014.ipb.ac.rs

# SIMULATION AND MODELING OF RESISTIVE PLATE CHAMBERS

D. Bošnjaković, Z.Lj. Petrović and S. Dujko

*Institute of Physics, University of Belgrade, Pregrevica 118, 11080 Belgrade, Serbia*

Due to their excellent timing resolution and good spatial resolution, Resistive Plate Chambers (RPCs) became one of the most commonly used gaseous particle detectors, mainly for timing and triggering purposes in high energy physics experiments. Despite of their simple construction, which often consists of a single gas gap between the electrodes of highly resistive material (e.g. glass or bakelite), their modeling is not an easy task. A complete model of these devices must consider three distinct physical processes: 1) primary ionization, i.e. interaction between the high energy particle and the gas, 2) charge transport and multiplication in the gas, and 3) signal generation and electrode relaxation effects. We focus on the first two processes and discuss their effects on the main performance characteristics of an RPC such as timing resolution and detection efficiency. Then, we review different approaches in RPC modeling. Finally, we present our "microscopic" RPC model where each electron and its collisions with the gas are followed using a Monte Carlo technique. This approach demands the use of high performance computing facilities and can be considered as a nearly exact model for relatively low values of signal threshold corresponding to about $10^6$ electrons in the gas gap. The results for timing resolution and efficiency of a specific timing RPC with 0.3 mm gas gap and a gas mixture of 85% $C_2H_2F_4$ + 5% iso-$C_4H_{10}$ + 10% $SF_6$ are compared with experimental values [1] while taking into account different cross section sets for electron scattering in $C_2H_2F_4$. The comparison is also made with an analytical model [2] for timing distribution of electron avalanches and possible causes of slight deviations are discussed.

**Acknowledgements:** This work is supported by MPNTR, Serbia, under the contract number OI171037.

## REFERENCES

[1] L. Lopes, P. Fonte and A. Mangiarotti, Nucl. Instrum. Meth. A 661, S194 (2012).
[2] W. Riegler, Nucl. Instrum. Meth. A 602, 377 (2009).

# STUDIES OF ELECTRON TRANSPORT IN GASES FOR RESISTIVE PLATE CHAMBERS

D. Bošnjaković, Z.Lj. Petrović and S. Dujko

*Institute of Physics, University of Belgrade,*
*Pregrevica 118, 11080 Belgrade, Serbia*

**Abstract.** We study the electron transport in gases used by Resistive Plate Chambers in ALICE, ATLAS and CMS experiments at CERN. Particularly, we identify and discuss the electron transport phenomena in these gases using the Boltzmann equation analysis and spatially resolved Monte Carlo calculations. The understanding of electron transport phenomena and its implications is necessary for correct implementation of transport data in modeling of these devices.

## 1. INTRODUCTION

Resistive Plate Chambers (RPCs) were introduced in 1980s as a practical alternative to spark counters with localized discharge [1,2]. Today, they are one of the most frequently used particle detectors in large high energy physics experiments owing to their outstanding timing resolution, good spatial resolution and low cost per unit volume while the electrodes of highly resistive material (e.g. glass or bakelite) make them resilient to destructive discharges [3]. They also found their way in other areas such as geophysics and medical imaging [4].

There were many approaches in modeling of RPCs. Being analytical, fluid or Monte Carlo based [5], they all require the knowledge of electron transport data in gases which are used as input parameters. Also, a matter of particular importance which had practically no attention in the particle detector community is the correct implementation of these data with respect to duality of transport coefficients. For example, in fluid modeling of these devices one must use the flux data but in models where electron avalanche is treated as a whole, bulk data must be used. In this work, we calculate the electron transport parameters and study the associated kinetic phenomena in gas mixtures used by RPCs in ALICE, ATLAS and CMS experiments at CERN.

## 2. THEORETICAL METHODS

Electron transport coefficients are calculated from the solution of the non-conservative Boltzmann equation (BE). Instead of the conventional two term approximation for solving the Boltzmann equation, we have used a

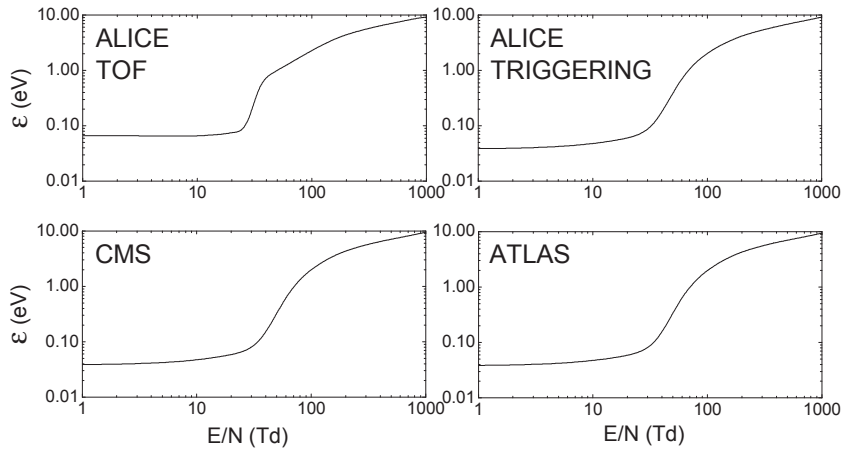


**Figure 1.** Variation of the mean energy with *E/N* for RPCs used in ALICE, CMS and ATLAS experiments at CERN.

contemporary multi term approach [6]. In addition to Boltzmann equation, a Monte Carlo technique is used to sample spatially resolved transport data; for more details the reader is refer to [7].

## 3. RESULTS AND DISCUSSION

The results in this section are calculated for the following RPC gas mixtures of $C_2H_2F_4$/iso-$C_4H_{10}$/$SF_6$, used at CERN: (1) ALICE timing RPC, 90/5/5; (2) ALICE triggering RPC, 89.7/10/0.3; (3) CMS triggering RPC, 96.2/3.5/0.3; and (4) ATLAS triggering RPC, 94.7/5/0.3. We use the cross section set for $C_2H_2F_4$ developed by our group [8], cross section for iso-$C_4H_{10}$ taken from MAGBOLTZ 2.7.1 code developed by S. Biagi [9], and cross sections for $SF_6$ taken from Itoh et al. [10]. The reduced electric field *E/N* is given in Td (1 Td = $1\times10^{-21}$ $Vm^2$).

Figure 1 shows mean electron energies over a range of *E/N* values, for different RPC gas mixtures used at CERN. We may observe a very small change of mean energy up to about 30 Td where the rapid rise begins. The small change of electron energy is due to the rising collision frequency for vibrational excitations in $C_2H_2F_4$. This effect can be named as *inelastic cooling* since the electrons loose considerable energy in inelastic collisions. At about 30 Td cross sections for vibration excitation begin to drop and electron energy starts to rise rapidly. In addition to inelastic cooling, for ALICE TOF mixture with higher $SF_6$ concentration, one can also observe that in the same *E/N* range the mean energy is significantly higher than the thermal value of 0.038 eV. This is a typical example of *attachment heating* [11] which takes place since electrons with lower energies are consumed in thermal attachment by the $SF_6$ molecules.

Calculations of drift velocities (Figure 2) reveal another interesting phenomenon: the bulk drift velocity in case of ALICE TOF mixture exhibits a

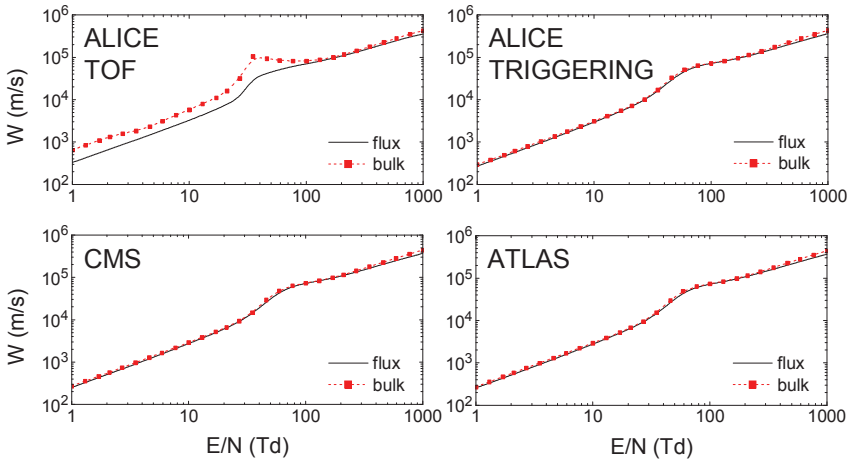


**Figure 2.** Variation of the bulk and flux drift velocities with *E/N* for RPCs used in ALICE, CMS and ATLAS experiments at CERN.

prominent negative differential conductivity (NDC) while this effect is not present in the flux component or in any other gas mixture. NDC is a kinetic phenomenon defined as a decrease of drift velocity with increasing electric field strength [12]. It arises from a certain combination of elastic and inelastic cross sections and is usually present in both flux and bulk components of drift velocity but it was argued whether it can be present only (or dominantly) in the bulk component when non-conservative collisions are present [13]. Here it is clear that the NDC is induced by electron attachment since it is not present in the flux component and the electron energies are well below the threshold for ionization. The occurrence of NDC can be understood in terms of spatially dependent (resolved) mean energy and attachment rate. It is well-known that the mean energy is not constant along the swarm because the electrons at the front of the swarm have higher energies than those at the back. This follows from the fact that electrons at the front gain more energy from the electric field as they are accelerated through a higher potential. As a consequence, the attachment rate coefficient is not uniform because the cross sections for attachment are energy dependent as well. In our case, the bulk drift velocity explicitly depends on the spatial profile of the attachment rate. Since the attachment rate is greater at the back of the swarm than at the front, the center of mass of the swarm shifts forward which results in an increase of bulk component of drift velocity over the flux component. This increase roughly depends on the spatial gradient (slope) of the attachment rate coefficient. Figure 3 shows the spatial profiles of attachment rate coefficients, for different *E/N* values, calculated using a Monte Carlo technique. One must bear in mind that calculations were performed for a stationary gas ($T$ = 0 K) and thus the values are shifted with respect to those obtained from BE so that the onset of NDC (the peak in the bulk drift velocity) corresponds to $E/N$ = 10 Td. Indeed, one can see that the slope is at its maximum for $E/N$ = 10 Td. With increasing $E/N$ the slope drops and so does the NDC.

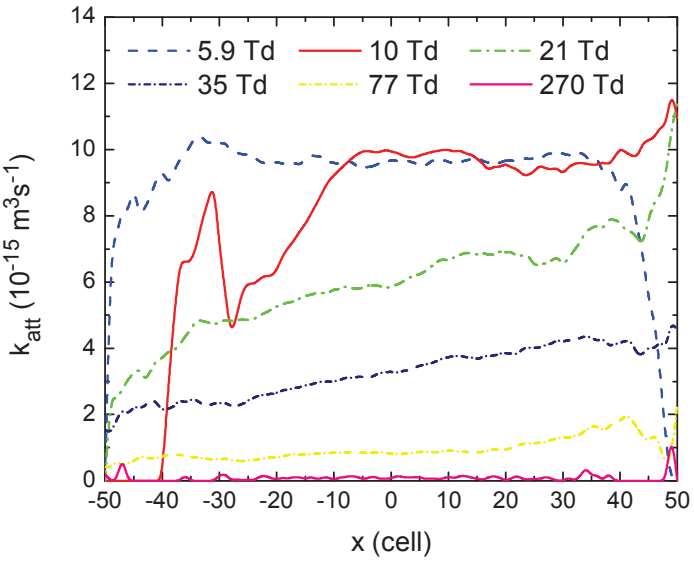


**Figure 3.** Spatially resolved attachment rate coefficient for a range of *E/N* in ALICE timing RPC. ($t$ = 1 ns)

## Acknowledgements

This work is supported by MPNTR, Serbia, under the contract number OI171037.

## REFERENCES

[1] R. Santonico and R. Cardarelli, Nucl. Instrum. Meth. 187, 377 (1981).
[2] R. Santonico et al., Nucl. Instrum. Meth. A 263, 20 (1988).
[3] P. Fonte, IEEE Trans. Nucl. Sci. 49, 881 (2002).
[4] M. Couceiro et al., Nucl. Instrum. Meth. A 661, S156 (2012).
[5] W. Riegler and C. Lippmann, Nucl. Instrum. Meth. A 518, 86 (2004).
[6] S. Dujko et al., Phys. Rev. E 81, 046403 (2010).
[7] Z. M. Raspopović et al., IEEE Trans. Plasma Sci. 39, 2566 (2011).
[8] O. Šašić et al., J. Phys. D: Appl. Phys. 46, 325201 (2013).
[9] S. Biagi, Nucl. Instrum. Meth. A 421, 234 (1999).
[10] H. Itoh et al., J. Phys. D: Appl. Phys. 26, 1975 (1993).
[11] R. E. Robson and K. F. Ness, Phys. Rev. A 33, 2068 (1986).
[12] Z. Lj. Petrović, R. W. Crompton and G. N. Haddad, Aust. J. Phys. 37, 23 (1984).
[13] S. B. Vrhovac and Z. Lj. Petrović, Phys. Rev. E 53, 4012 (1996).

ISBN 978-86-7031-244-9


26th Summer School and International
**S**ymposium on the **P**hysics of **I**onized **G**ases

August 27th -31st, 2012, Zrenjanin Serbia

# CONTRIBUTED PAPERS & ABSTRACTS OF INVITED LECTURES AND PROGRESS REPORTS



**Editors**
**M. Kuraica, Z. Mijatović**

**University of Novi Sad, Faculty of Sciences**
**Department of Physics**
**Novi Sad, Serbia**

# ELECTRON TRANSPORT COEFFICIENTS IN GASES FOR RESISTIVE PLATE CHAMBERS

D. Bošnjaković, S. Dujko and Z.Lj. Petrović

*Institute of Physics, University of Belgrade,*
*Pregrevica 118, 11080 Belgrade, Serbia*

**Abstract.** Electron transport coefficients for electron swarms in isobutane, $C_2H_2F_4$ and their mixtures are calculated using a Monte Carlo simulation technique and a multi term solution of non-conservative Boltzmann equation. Values of drift velocity and rate coefficients are reported here. Results can be used as input parameters for simulation-aided design and optimization of Resistive Plate Chambers.

## 1. INTRODUCTION

Introduced in 1980s, Resistive Plate Chambers (RPCs) [1,2] quickly became a widely used gaseous particle detector in high energy physics experiments mainly because of their simple construction, good rate capability, and timing resolution. They can also have a benefit of high position resolution which makes them a good alternative to scintillator and solid state detectors used in medical imaging applications [3].

Since their introduction, several gas mixtures have been proposed and tested with the goal of achieving optimum performance characteristics such as efficiency and timing. Isobutane ($iC_4H_{10}$) and Freon 134a ($C_2H_2F_4$) are the most frequently used gases in RPCs. They have good quenching and streamer suppression properties. The mixture of $C_2H_2F_4$ and isobutane, with a small addition of $SF_{6,}$ is usually used in RPCs at the CMS, LHCb and ALICE experiments.

During last 15 years, several numerical simulations of RPC's operation have been performed [4-7]. They have been meant to give an insight into the underlying physical phenomena (by comparison with experimental measurements) and to be used as a tool for detector design and optimization. Electron swarm properties including the drift velocity, diffusion tensor, and ionization and attachment coefficients were input parameters in these simulations.

In this work, as a first step in our ongoing investigation on RPCs we present electron transport coefficients in isobutane, $C_2H_2F_4$ and in their mixtures as a function of reduced electric field strength *E/N*. Results are obtained using a

Monte Carlo simulation technique and multi term Boltzmann equation analysis. Our results are compared with experimental data when possible and with those obtained by the MAGBOLTZ simulation program [8].

## 2. METHODS

In this work we apply Monte Carlo simulation technique and multi term solution of non-conservative Boltzmann equation. Computer codes behind of these methods are verified for a number of benchmarks [9,10]. In the present Monte Carlo code we follow a large number of electrons (typically $10^4$-$10^6$) over small time steps. The electron swarm is assumed to develop in an infinite gas under uniform fields. All calculations are performed for zero gas temperature. It is assumed that all electron scattering is isotropic. After relaxation to a steady-state, all transport properties are averaged over the time in order to obtain better statistics. The reader is referred to a recent review [10] for a detailed discussion of the multi term Boltzmann equation solution technique.

For comparison, electron transport coefficients are calculated by the MAGBOLTZ [8], a Monte Carlo simulation tool which is well known in gaseous particle detector community. MAGBOLTZ uses its own cross section database which is imbedded in the code. For calculations made by our codes, we have employed MAGBOLTZ's set of cross sections for isobutane as no other cross section sets for isobutane exist [11]. For $C_2H_2F_4$, however, we have used a cross section set recently developed by our group [12].

## 3. RESULTS AND DISCUSSION

In this work we consider the electric field strength range:1-1000 Td (1 Td = $10^{-21}$ $Vm^2$). Typical RPC operating field strengths are between 200 and 500 Td. The gas number density is $3.54\times10^{22}$ $m^{-3}$ which corresponds to the pressure of 1 Torr at 273 K. Here, we present only those results which could be directly compared to experimental data obtained in a narrow *E/N* range, usually using RPC-like configuration for measurement.

Figure 1 (left) shows our Monte Carlo results for the ionization coefficient in isobutane. Our results are compared with the MAGBOLTZ calculations and experimental data. We see that our results mostly agree with those from MAGBOLTZ except for higher and/or lower electric fields. Experimental data from Nakhostin *et al.* [13] for higher electric fields fit quite well with our calculations while those from Lima *et al.* [14] for lower electric fields are closer to MAGBOLTZ's predictions.

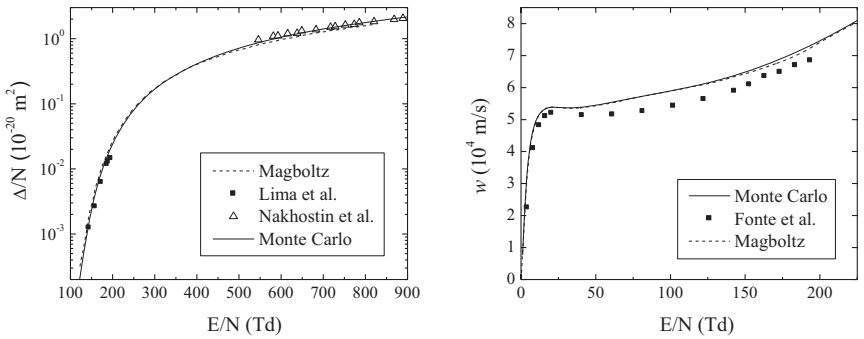


**Figure 1.** Variations of the first Townsend ionization coefficient ( left) and drift velocity (right) with *E/N* in isobutane.

In Figure 1 (right) we show the variation of the drift velocity with *E/N* in isobutane. Our results are compared with those obtained by the MAGBOLTZ and with the experimental data taken from Fonte *et al.* [11]. For *E/N* between 1 and 225 Td, calculations performed by our Monte Carlo code show no differences between the flux and bulk drift velocity components. Our results agree quite well with those obtained from MAGBOLTZ, except between 150 and 200 Td. On the other hand, the experimental data for higher field strengths do not fit well to numerical calculations. Reported systematic errors in this range are about 10% which questions the quality of the experimental technique.

In Figure 2 we display the drift velocity in $C_2H_2F_4$-isobutane mixture (90-10%) as a function of *E/N*. Calculations are performed by a multi term theory for solving Boltzmann's equation and compared with those obtained by the MAGBOLTZ and with measurements by Colucci *et al.* [15]. It is evident that our results strongly disagree with those from MAGBOLTZ. This can be

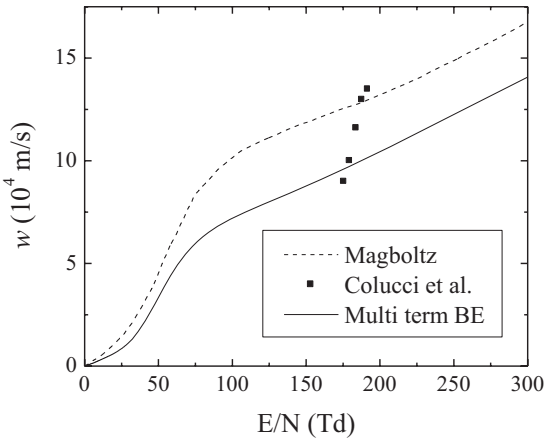


**Figure 2.** Variation of the drift velocity with *E/N* in $C_2H_2F_4$-isobutane gas mixture (90-10%).

attributed to different cross sections used for $C_2H_2F_4$. We see that the measurements do not fit well to either our or MAGBOLTZ results.

From this work we see that discrepancies between the measured swarm parameters and those calculated using the independently assessed cross section sets may be due to several causes: (1) uncertainties in the cross sections; (2) uncertainties in the measured swarm parameters; and (3) due to the effects of collisions between electrons and excited molecules. Much remains to be done in order to improve the existing sets of cross sections for gases of interest for RPCs.

## Acknowledgements

This work is supported by MPN, Serbia, under the contract number OI171037.

## REFERENCES

[1] R. Santonico, R. Cardarelli, Nucl. Instr. and Meth. 187, 377 (1981).
[2] R. Santonico, R. Cardarelli, A.D. Biagio, A. Lucci, Nucl. Instr. and Meth. A 263, 20 (1988).
[3] A. Blanco, N. Carolino, C.M.B.A. Correia, R. Ferreira Marques, P. Fonte, D. González-Díaz, A. Lindote, M.I. Lopes, M.P. Macedo, A. Policarpo, Nucl. Instr. and Meth. A 533, 139 (2004).
[4] M. Abbrescia, et al., Nucl. Phys. B 78, 459 (1999).
[5] W. Riegler, C. Lippmann, R. Veenhof, Nucl. Instr. and Meth. A 500, 144 (2003).
[6] S.H. Ahn, et al., Nucl. Instr. and Meth. A 533, 32 (2004).
[7] L.K. Khorashad, et al., Nucl. Instr. and Meth. A 628, 470 (2011).
[8] S. Biagi, Nucl. Instr. and Meth. A 421, 234 (1999).
[9] Z.M. Raspopović, S. Sakadžić, S. Bzenić and Z.Lj. Petrović, IEEE Trans. Plasma Sci. 27, 1241 (1999).
[10] S. Dujko, R.D. White, Z.Lj. Petrović and R.E. Robson, Phys. Rev. E 81 046403 (2010).
[11] P. Fonte, A. Mangiarotti, S. Botelho, J.A.C. Goncalves, M. Ridenti, C.C. Bueno, Nucl. Instr. and Meth. A 613, 40 (2010).
[12] O. Šašić, et al., (2012), unpublished.
[13] M. Nakhostin, M. Baba, T. Ohtsuki, T. Oishi, T. Itoga, Nucl. Instr. and Meth. A 572, 999 (2007).
[14] I.B. Lima, et al., Nucl. Instr. and Meth. A 670, 55 (2012).
[15] A. Colucci, et al., Nucl. Instr. and Meth. A 425, 84 (1999).

# XII workshop on Resistive Plate Chamber and Related Detectors

**Sunday 23 February 2014 - Friday 28 February 2014**

**Beijing**

# Book of abstracts

**poster / 46**

## Electron transport phenomena in gases for RPCs

BOŠNJAKOVIĆ, Danko [1]; PETROVIĆ, Zoran Lj. [1]; DUJKO, Saša [1]

[1] *Institute of Physics, University of Belgrade*

**Corresponding Author**: dbosnjak@ipb.ac.rs

The progress and further improvements of Resistive Plate Chambers (RPCs) require the most accurate modeling of electron transport processes in the gas mixtures of C2H2F4, i-C4H10, SF6 and rare gases. In this work we first focus on the availability of data for electron collisional processes in relevant gases with particular emphasis on C2H2F4. We present recently developed set of cross sections for electron scattering in C2H2F4 and then from the solution of non-conservative Boltzmann equation we investigate electron transport in mixtures of C2H2F4, i-C4H10, and SF6 under swarm conditions required for fluid modeling of RPC detectors in streamer mode. Calculations are performed over a range of E/N values and C2H2F4 concentrations relevant to both timing and triggering modes of RPCs operation. Values and general trends of mean energy, drift velocity and diffusion tensor as well as rate coefficients for different collisional processes including the ionization and electron attachment are presented in this work.
We then discuss, in particular, (1) the explicit modification of transport coefficients by non-conservative collisional processes of attachment and ionization; (2) the accuracy of the two term approximation for solving Boltzmann's equation; (3) the correct implementation of transport data in modeling of RPCs; and (4) the differences between the steady-state Townsend and hydrodynamic transport properties. In addition, using a Monte Carlo simulation technique we investigate the spatiotemporal development of electron avalanches under the conditions typically found in RPCs to facilitate understanding of the non-local electron kinetics in these detectors.

**poster / 47**

## Simulation of RPCs using microscopic Monte Carlo technique

BOŠNJAKOVIĆ, Danko [1]; PETROVIĆ, Zoran Lj. [1]; DUJKO, Saša [1]

[1] *Institute of Physics, University of Belgrade*

**Corresponding Author**: dbosnjak@ipb.ac.rs

We present a model for time response of Resistive Plate Chambers (RPCs) based on a 3D microscopic approach. Individual electrons and their collisions with the background gas are followed in a typical Monte Carlo fashion. Because of limited computing resources, a relatively low value of signal threshold is chosen which corresponds to about one million electrons. This is still beyond space-charge effects. Timing resolution and efficiency are calculated for a specific timing RPC: 0.3 mm gas gap and a gas mixture of 85% C2H2F4 + 5% i-C4H10 + 10% SF6. Results are obtained for a range of electric field strengths, different primary ionization models and different sets of cross sections for electron scattering in C2H2F4. Contrary to an analytical model, it is shown that the timing resolution does not depend solely on the effective ionization rate but rather on the cross section set as a whole. Comparison is also made with experimental values from Lopes et al. (2012) and good agreement is found.

EMS

# XVIII International Symposium on Electron-Molecule Collisions and Swarms

## Programme and Book of Abstracts


XVII International Workshop on Low-Energy Positron and Positronium Physics &
XVIII International Symposium on Electron-Molecule Collisions and Swarms
19 - 21 July 2013, Kanazawa, Japan

POSMOL 2013

TE-06

# Non-conservative electron transport in gases and its application in modelling of non-equilibrium plasmas and particle detectors

**S. Dujko[1,2], D. Bošnjaković[1], J. Mirić[1], Z.Lj. Petrović[2], R.D. White[3], A.H. Markoyan[2] and U. Ebert[2]**

[1]Institute of Physics, University of Belgrade, Pregrevica 118, Zemun 11080, Serbia

[2]Centrum Wiskunde & Informatica, (CWI), P.O. Box 94079, 1090 GB Amsterdam, The Netherlands

[3]ARC Centre for antimatter-Matter Studies, School of Engineering and Physical Sciences, James Cook University, Townsville 4810, Australia

sasa.dujko@ipb.ac.rs, S.Dujko@cwi.nl

The advancements in modern day technology associated with non-equilibrium plasma discharges depend critically on accurate modeling of the underlying collision and transport processes of charged particles in gases. To meet these challenges, we have undertaken a program to understand the kinetic behavior of charged particles under the combined action of electric and magnetic fields in neutral gases. A multi term theory for solving the Boltzmann equation has been developed and used to calculate transport coefficients of charged-particle swarms in neutral gases [1,2].

In the first part of this talk I will focus on non-equilibrium magnetized plasma discharges where the electric and magnetic fields can vary in space, time and orientation depending on the type of discharge and where attention must be paid to the correct treatment of temporal and spatial non-locality within the discharge. I will highlight the duality of transport coefficients arising from the explicit effects of non-conservative collisions particularly for electrons in rare gas metal-vapor mixtures, having in mind applications in lighting industry. As an example of fluid modeling of plasmas, I will discuss the recently developed high order fluid model for streamer discharges [3,4]. Starting from the cross sections for electron scattering, it will be shown how the corresponding transport data required as input in fluid model should be calculated under conditions when the local field approximation is not applicable. The temporal evolution of electron number density and electric field in the classical first order and in the high order model are compared and the differences will be explained by physical arguments.

In the second part of this talk I will discuss the detector physics processes of resistive plate chambers that are often used in many high energy physics experiments. Critical elements of modeling include the primary ionization, avalanche statists and signal development. The Monte Carlo simulation procedures that implement the described processes will be presented. Time resolution and detector efficiency are calculated and compared with experimental measurements and other theoretical calculations.

**References**

[1] S. Dujko, R.D. White, Z.Lj. Petrović and R.E. Robson, Phys. Rev. E **81** 046403 (2010)
[2] R.D. White, R.E. Robson, S. Dujko, P. Nicoletopoulos and B. Li, J. Phys. D: Appl. Phys. **42** 194001 (2009)
[3] S. Dujko, A. Markosyan, R.D. White and U. Ebert, under revision for J.Phys.D.
[4] A. Markosyan, S. Dujko and U. Ebert, under revision for J.Phys.D.

E-04

# Monte Carlo modelling of resistive plate chambers

**D. Bošnjaković[1], Z.Lj. Petrović[1] and S. Dujko[1,2]**

[1]Institute of Physics, University of Belgrade, Pregrevica 118, 11080 Zemun, Serbia

[2]Centrum Wiskunde & Informatica (CWI), P.O. Box 94079, 1090 GB Amsterdam, The Netherlands

sasa.dujko@ipb.ac.rs, S.Dujko@cwi.nl

In this work we discuss the basic elements of modeling of the Resistive Plate Chambers (RPCs) often used in many high energy physics experiments for timing and triggering purposes [1,2]. These detectors consist of one or more gas gaps between resistive or metallic electrodes and usually with signal-transparent high-voltage electrodes, isolating layers, and different arrangements of signal pickup electrodes. RPCs can be operated in avalanche mode and in streamer mode with time resolutions down to 50 ps. In spite of their simplicity, modeling of RPCs is a very challenging task due to existence of complex phenomena occurring in very different time-scales ranging from pico to milli seconds.

First, we focus the availability of data for electron collisional processes in $C_2H_2F_4$ [3,4], iso-$C_4H_{10}$ and $SF_6$, typically used in the RPC gas mixtures. We present recently developed set of collisional and transport data for electrons in the gas mixtures used in RPCs. Electron transport coefficients required for fluid modeling of these detectors in streamer mode are calculated from solution of the non-conservative Boltzmann equation [5]. We then discuss, in particular, (1) the explicit modification of transport coefficients about by non-conservative collisional processes of attachment and ionization; (2) the accuracy of the two term approximation for solving Boltzmann's equation; and (3) the correct implementation of transport data in modeling of RPCs; and (4) the differences between the steady-state Townsend and hydrodynamic transport properties. In addition, we investigate the spatiotemporal development of electron swarms in the presence of electric field to facilitate understanding spatial non-locality of electron kinetics in these detectors.

Second, we present our Monte Carlo model for timing RPCs. We have calculated the time-response of these detectors operated in avalanche mode. The development of induced signal was simulated for a specific timing RPC geometry (0.3 mm gas gap, one glass and one metallic electrode). The time-resolution and efficiency were calculated by signal discrimination with a given threshold. Calculations were made for different gas mixtures and for a range of electric fields. The results agree very well with the experimental measurements. The primary ionization, made by a high-energy particle travelling through the detector, was included using a well known probability model with the available data for mean distance between electron clusters and cluster size distribution, assuming minimum ionizing particles.

**References**

[1] W. Riegler and C. Lippmann, Nucl. Instrum. Meth. A 518 **86** (2004)
[2] P. Fonte, IEEE Trans. Nuclear Sci. **49** 881 (2002)
[3] J. de Urquijo, A.M. Juárez, E. Basurto and J.L. Hernández-Ávila, Eur. Phys. J. D **51** 241 (2009)
[4] O. Šašić, S. Dupljanin, J. de Urquijo and Z.Lj. Petrović, accepted for publication in J.Phys.D.
[5] S. Dujko, R.D. White, Z.Lj. Petrović and R.E. Robson, Phys. Rev. E **81** 046403 (2010)

Journal of Physics: Conference Series **488** (2014) 012047 doi:10.1088/1742-6596/488/1/012047

# Kinetic Phenomena in Transport of Electrons and Positrons in Gases caused by the Properties of Scattering Cross Sections

**Zoran Lj. Petrović[1,2,7], Srđan Marjanović[1], Saša Dujko[1], Ana Banković[1], Olivera Šašić[1], Danko Bošnjaković[1], Vladimir Stojanović[1], Gordana Malović[1], Stephen Buckman[3], Gustavo Garcia[4], Ron White[5], James Sullivan[3] and Michael Brunger[6]**

[1] Institute of Physics, University of Belgrade, POB68 11080 Zemun Serbia
[2] Academy of Sciences and Arts of Serbia, 11001 Belgrade Serbia
[3]Centre for Antimatter-Matter Studies (CAMS), Research School of Physics and Engineering, Australian National University, Canberra, ACT, Australia
[4] Instituto de Fısica Fundamental, Consejo Superior de Investigaciones Cientıficas (CSIC), 28006 Madrid, Spain
[5] CAMS, School of Engineering and Physical Sciences, James Cook University, Townsville QLD, Australia
[6] CAMS, CaPS, Flinders University, G.P.O. Box 2100, Adelaide SA 5001, Australia

E-mail: zoran@ipb.ac.rs

**Abstract**. Collisions of electrons, atoms, molecules, photons and ions are the basic processes in plasmas and ionized gases in general. This is especially valid for low temperature collisional plasmas. Kinetic phenomena in transport are very sensitivitive to the shape of the cross sections and may at the same time affect the macroscopic applications. We will show how transport theory or simulation codes, phenomenology, kinetic phenomena and transport data may be used to improve our knowledge of the cross sections, our understanding of the plasma models, application of the swarm physics in ionized gases and similar applications to model and improve gas filled traps of positrons. Swarm techniques could also be a starting point in applying atomic and molecular data in models of electron or positron therapy/ diagnostics in radiation related medicine..

## 1. Introduction

In this paper we present a survey of some of the recent results of the physics of swarms of charged particles (we will confine our interest to electrons and positrons). Our first and necessary point is to illustrate some of the recent results obtained by the group(s) at the Institute of Physics in Belgrade (together with our collaborators). We also wish to illustrate

[7] To whom any correspondence should be addressed. ZLjP wishes to acknowledge that Ministry of Education, Science and Technology of Serbia (OI171037 and III41011) and Serbian Academy of Arts and Sciences (SANU 155) have, provided a partial support to the ongoing activities of the group in Belgrade but none for the participation at the conference or preparation of the manuscript.

how swarm physics connects on one side to atomic and molecular collisions (and thus to overall atomic and molecular physics) and on the other to non-equilibrium plasmas and their numerous applications. As the topic of swarms has not been addressed frequently at ICPEAC (although one of its satellites, Electron-molecule Collisions and Swarms, covers the topic very well) this presentation will necessarily be rather broad but not very detailed.

Collisions of electrons, atoms, molecules, photons and ions are the elementary processes occurring in plasmas. It may be argued that the level of individual collisions is the most fundamental level of phenomenology required to describe non-equilibrium collisional plasmas. That is so for two principal reasons: the first being that the duration of the collisions is many orders of magnitude shorter than the mean free time between the collisions. Thus we may bury all the quantum mechanics into the cross sections and basic properties of the energy levels and molecules. As a result, we may even use classical trajectories for charged particles and thus the Monte Carlo technique has had so much success. The second reason is related to the first and it is that the De Broglie's wavelength of particles is usually small compared to the mean volume per particle in the gas, at least until we reach very high densities (e.g. as in liquids). Thus electrons collide with only one target per collision.

A reductionist view of the science which dominated in the past declared that the more basic the phenomena were, the more fundamental they were. In that view of the world, the field theory and mathematics on their own may explain the psychological states of humans! A more realistic view which, luckily, prevails today is that there are layers of phenomenology, each with its own rules and foundations and each providing its accomplishments that are not trivially predicted at the more basic levels. In this way we may construct a path between atomic and molecular physics and the numerous modern applications of low temperature plasmas. As previously mentioned, there is no need to go deeper than the physics of collisional processes (including a range of collisions with surfaces). The next stage is the physics of swarms where collisions join the statistical physics and kinetic theory in addition to the surface processes. More detailed presentations of this realm of physics have been given in earlier texts [1,2], while more recent reviews have been given in references [3-5]. It is possible to say that little in the papers presenting the cross section data prepares us for the complex kinetic phenomena that evolve in the swarm physics, such as negative differential conductivity or negative absolute mobility [6,7].

The next layer of phenomenology is that of low temperature or more accurately non-equilibrium plasmas (NEP). It brings in space charge and other plasma effects, chemistry and many more different inputs. Swarm physics, represented by its kinetic phenomena, together with atomic collision data are the building blocks of the NEPs but little prepares us for the phenomena such as the spewing of the plasma bullet (ionization front) from the glass tube where an atmospheric pressure plasma jet (APPJ) is formed [8,9]. This device often produces a plasma bullet (ionization front) that actually moves faster, and is bigger and brighter, in the supposedly hostile world of atmospheric gases once it leaves the region of high field between the electrodes wrapped around the tube where more favourable gases for its formation dominate. But even at this level one cannot really envisage why and how such plasmas may induce, for example, preferential differentiation of human (periodontal ligament mesenchymal) stem cells into one out of four possible types of the cells [10].

Finally, one should welcome another change in the attitude that happened recently. It has been slightly over 100 years since the discovery of electron. Its discoverer J.J. Thompson toasted at Christmas receptions: ″To the electron and may nobody find its application.″. Needless to say, the previous century being labeled as the century of the electron means that some applications were eventually found. The attitude that applied is not fundamental has, however, changed. Luckily non-equilibrium plasmas offer one of the quickest and most abundant fronts of development of new applications and each application brings in requirements for new phenomena to be included. For example, attempting to apply NEPs to

medicine requires an understanding of a large part of the relevant medical knowledge. Following publication of a major review by David Graves, of the mechanisms coupling reactive species from the plasmas with biological triggers [11], there is now no room for plasma and atomic physicists to claim that medical processes need not be understood from their viewpoint, they simply have to learn them (Latin terms and all). Nevertheless one could claim that at the deepest relevant level leading to such applications, one may find atomic and molecular collisions however remote from the final outcome those may be [10].

## 2. Electron swarms in gases, cross section data sets and kinetic phenomena

Swarms may be simply defined as ensembles of particles (in this case electrons and positrons) moving in the background gas under the influence of external fields (if charged), limited by the walls of the vessel. These particles do not suffer effects of any significance due to interactions between themselves (Coulomb force, shielding of the external field) and also have negligible chances of colliding with the remnants of previous collisions. In other words, they move in the external fields affected mainly by the collisions with the pristine background gas.

Swarms bring transport theory and other aspects of statistical physics to the table, and often effects of surfaces may be needed albeit only in specific situations (e.g. a Steady State Townsend experiment). The transport may be well represented by a single particle distribution function, so the standard Boltzmann equation (BE) is appropriate. However, due to 7 degrees of freedom, a complex theoretical treatment is required for solving the BE. Due to the complexity of the cross sections (the dependence on the energy that can only be tabulated) and hence collision operator, the final result has to be obtained numerically. The resulting energy distribution function is however not something that can be measured, and the swarm physics focuses on averaged properties such as transport coefficients (drift velocity, diffusion tensor, ionization coefficients) or rates for specific processes (excitation or chemical).

Initially swarm physics was developed when techniques of electrochemistry were applied to study properties of charged particles in gases, especially when their elementary nature became obvious. However, they quickly proved to be a very good source of data for cross sections for the dominant processes especially after numerical solutions to the BE became available. The advantage of the technique was originally significant, as it provided good absolute calibration, and results for He were only matched by theory and beam techniques some ten to twenty years later [1]. Most importantly, if a full set of swarm facilities is used the resulting cross section set provides good number, momentum and energy balances for the charged particles in the gas and is thus directly applicable in the modeling of plasmas.

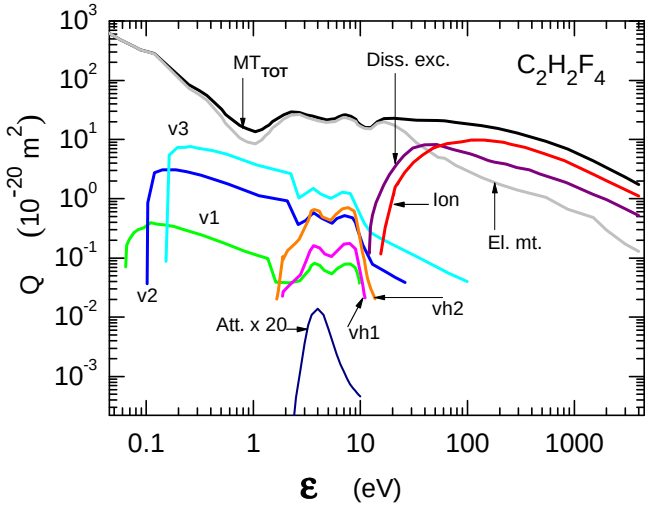


**Figure 1**. The cross section set for $C_2H_2F_4$ [12], MT- total momentum transfer, v-vibrational modes, Att-attachment, ion-ionization, El mt elastic momentum transfer, Diss. Exc. Dissociative excitation..

Recent swarm derived cross section sets cover many gases so we shall give only one example, for the 1,1,1,2-tetrafluoroethane ($C_2H_2F_4$) molecule [12]. Transport coefficients measured by a Pulsed Townsend technique were converted to cross sections, based on an initial set that was available in the literature due to S. Biagi. Results are shown in Figure 1.

A disadvantage of the swarm technique is that it is indirect i.e. it involves guessing of the cross section set and then comparing the calculated transport coefficients to the experimental data until agreement is

reached. In addition its resolution is poor, especially at higher energies, and the results potentially suffer from non-uniqueness.

Reliable results are usually obtained from drift velocities and characteristic energies (diffusion coefficient divided by mobility) for energies up to 1 – 2 eV, while typical electron energies in relevant plasmas are higher. If the ionization coefficient is used in the analysis one may extend the energy range of the set. Assuming that the measured ionization cross sections are very accurate we can fit the ionization rate by adjusting the middle range electronic excitation cross sections or dissociation to the ground state (which are often incomplete).

The accuracy of the resulting cross sections depends very much on the accuracy of the transport theory (or the corresponding Monte Carlo simulation (MCS). Numerous tests need to be made to check the codes against specially designed benchmarks, for various aspects of the transport or properties of the processes [13]. On the other hand one needs to reopen, in a systematic fashion, the issue of anisotropic scattering. At low energies, due to the randomizing effect of frequent collisions, isotropic scattering is a good approximation provided that the momentum transfer cross section was obtained with that approximation. It has been shown, however, that for mean energies in excess of 20 eV or even for smaller energies when inelastic processes are very strong, one needs to include differential cross sections i.e. a full anisotropic model.

A plethora of atomic and molecular processes acting at the same time, that use up the energy gained from the field, leads to the formation of the shape of the electron energy distribution function (EEDF), and furthermore, but less obviously to the dependencies of the averaged properties, i.e. the transport and rate coefficients. Those processes finally lead to the functionality of low temperature plasmas and their many applications. From the viewpoint of fundamental physics the most interesting aspect of the swarm physics are the so-called kinetic phenomena [3,5]. Those represent an often counter intuitive behaviour of the collective properties, that cannot be predicted from the individual trajectories or from the shape of the cross sections (at least not without some experience). Those may be loosely classified according to the primary source of their existence (although the cross section magnitudes, shapes and properties are generally relevant) :

- **Dependence on the rates of momentum transfer and inelastic processes:** anisotropic diffusion; diffusion heating/cooling; enhanced mobility; negative differential conductivity (NDC); spatial separation of fast and slow particles-i.e the energy gradient, ...
- **Non conservative transport:** attachment heating/cooling; negative absolute mobility; difference between flux and bulk transport coefficients; positron NDC for bulk drift; skewed Gaussians, …
- **Magnetic field induced:** magnetic field cooling; ExB drift; ExB anisotropy of diffusion,...
- **NDC for positrons in liquids**
- **Time dependent fields:** anomalous diffusion; limited relaxation; phase delays at high frequencies; time resolved NDC; transient negative diffusivity, heating of electrons due to cyclotron-resonance effects,,..
- **Non-hydrodynamic:** Frank Hertz oscillations and Holst Oosterhuis structures; runaway ions; runaway electrons; thermalization/equilibration (non-local transport); increasing mean energies close to the boundaries; back-diffusion.

The fundamental reasons for these effects lie in the interplay between the times or spatial scales required for relaxation of number, momentum and energy, and in the interplay between the source of energy and momentum (i.e. the external field) and the processes that dissipate those properties. One example of kinetic phenomena is particularly important for the world of Atomic and Molecular physics. Absolute negative mobility has been predicted by several authors. The phenomenological explanation requires a group of electrons to be released with energy of 2 eV in a mixture of argon with 0.5% of $F_2$ (or any other gas with a large thermal attachment). The majority of the electrons would be accelerated by the field and would have an increasing chance to collide. If scattering is isotropic then 50% of the electrons will scatter backwards and join the smaller group of electrons that move against the field. Although those lose energy, the decreasing cross section will reduce their chances of

redirection until they thermalize in the region of the Ramsauer Townsend (RT) minimum. There, the electric field would again accelerate the majority of the electrons in the expected direction. Thus, for a while, electrons would on average move against the field and current – mobility would be negative. If one adds small amount of $F_2$ the thermal attachment will eat up the thermalized electrons not allowing them to accelerate and the current would be negative perpetually [14,15]. Of course it has been shown that this does not mean that we have a source of free energy although entropy is in principle reduced. However we pay the price by producing a lot of negative ions which contribute to an even greater growth of entropy [16]. The importance of this example is that it provides a situation where atomic processes may be used to tailor the distribution function, and in essence act as Maxwell's demon (in this case the thermal attachment). It is also not a man made device. Requirement to maintain the second law of thermodynamics requires us to separate at least two kinds of transport coefficients. For drift velocities we may have an average over all electrons in all of the space (the flux drift velocity), while we may also follow the center of the mass of electrons and determine its velocity (the bulk drift velocity). The distinction between these two is due to the changing number of particles (non-conservative processes; attachment, postronium (Ps) formation for positrons or ionization for electrons) and the difference may be associated with the vailidity of the second law of thermodynamics [16].

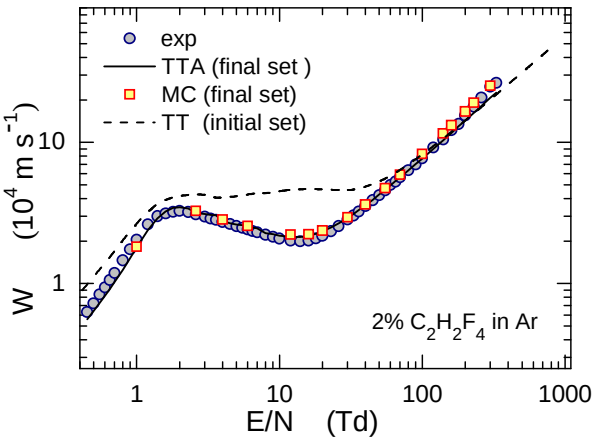


**Figure 2**. Fit of the experimental drift velocities (open circles) in $C_2H_2F_4$ with cross sections from figure 1 [12] (solid circles and line) and with an older set that was previously in use (see [12]). NDC is well developed between 2 Td and 20 Td.

We shall also show one example of the related phenomenon of negative differential conductivity (NDC), where drift velocity is reduced as the field increases and the mean energy increases due to the reduced control of the energy by inelastic process and increased randomization of directions in momentum transfer collisions. This example also shows how the structure in the drift velocity may be used to improve the uniqueness of the cross sections, as the calculations with another, similar, set does not show the experimentally observed NDC [12].

Kinetic phenomena, being shaped by the cross sections, provide an opportunity to strengthen the ability to normalize the cross section sets and also to modify and even define some of the applications or plasma properties. Thus those effects should be recognized and their implications understood when one wants to model collisional NEP.

## 3. Direct application of swarm data and models in the physics of ionized gases

In some cases when space charge is not excessive, swarms may be used as a direct representation of the ionized gas (often under those conditions, however, all conditions are not met to call such systems a plasma). The first example is the physics of Townsend discharges. The fact that swarm models are exact for such circumstances (in the limit of vanishingly small currents), makes them perfect to determine atomic and molecular processes in gas phase [17] and on surfaces and to study gas breakdown as well sometimes even revealing new phenomena in experimental observations [18]. Further direct application of swarm data and theory is in attempts to optimize gaseous dielectrics. In principle, two directions of research are dominant. The first is replacing $SF_6$ by more ecologically acceptable gases and the second is to produce mixtures of such gases that would allow their operation without the need for expensive high pressure vessels.

Another direction of research where swarm models and data are used abundantly (albeit that field has almost severed its connections with the swarm community) is that of the gas filled particle

detectors, including the nowadays most popular Resistive Plate Chambers (RPC)[19]. Using the Monte Carlo code developed to study swarms and obtain cross sections, and the newly established cross section set, we were able to calculate the time response of such devices [20] that agrees well with experiments. These results may nowbe used to optimize gas mixtures, operating conditions, chemistry and control the degree of ionization to speed up the counting rate. Other types of gas filled detectors may be modeled in a similar fashion.

The most important aspect in application of swarm physics, is in so called low temperature plasmas (we prefer to call them non equilibrium plasmas-NEP). We could spend much space on this issue, but it is only covered here as a brief introduction with more being found in reference [21]. The kinetic theory and the transport data all enter fluid models and together with the solution for the field distribution are the foundation of the theory. The hybrid models use the same data together with the cross section sets **that have to be complete** and thus be tested by the swarm technique, as do the kinetic codes. As one example we can describe capacitively coupled RF plasmas, which have sheaths close to the electrodes and with high fields that increase on one side and decrease on the other. During the reduction of the field electrons diffuse into that region and get accelerated into the plasma when the field starts increasing again. The diffusion flux of electrons is defined by the longitudinal diffusion coefficient, the one that shows anomalous behavior due to inability of the electron energy to respond the changes in the fields. This inability follows from the finite relaxation time of the electron energy which is strongly affected by the shape of the elastic cross section. On the other hand, for inductively coupled RF plasmas the ExB drift opens new channels to feed energy into the plasma [3]. Most models however assume constant (in space and time) transport coefficients, and neglect additional components of drift velocity and diffusion when magnetic fields are present. Nevertheless it has been difficult to impress upon the plasma modeling community that their models, when applied to simple low space charge limit benchmark situations, **should be able to replicate the swarm benchmarks**. Completing this exercise, however, would open many issues on the available cross sections and would forge a stronger link between atomic and molecular collision physics and the plasma modeling community. At the same time it would make binary collision experts aware of the data needs for the numerous plasma applications,

Another issue is that of the pertinent theory. As mentioned above, most frequently spatial and temporal uniformity are assumed in modeling. This is seriously wrong in cases of sharp gradients, in the profiles of plasma properties when hydrodynamic expansion of the theory is not an option (and is still being used in almost all cases). One such example is that of the streamers. Streamers are the basis for most high pressure discharges and recently a theory has been developed that includes proper treatment of transport across strong gradients in various streamer properties. Although the space charge made the final profile very robust, the improved theory produced results that had a significant change in the speed of propagation [22]. Streamers are an essential component of a number of atmospheric plasmas including lightning, sprite discharges in the upper atmosphere and atmospheric pressure plasma jets, which are being championed for novel medical procedures while having some intriguing physics on their own [8]. Other atmospheric discharges like aurora are often modeled [23] by using measured distribution functions from the atmosphere, in a procedure that resembles swarm models. It seems possible that a similar analysis should be made with distribution functions calculated having in mind all the available data and conditions at high altitudes.

## 4. Positrons in gases: swarms and (swarms in) traps

The absence of swarm experiments for positrons, with two exceptions [24], made us adopt a strategy that we do not advise for electrons. That is to collect the available cross sections, which are now generally available for several of the most important gases [25-27], and calculate the transport coefficients hoping to identify new kinetic phenomena that would justify building new swarm experiments. It was found that for gases with a strong positronium formation cross section, skewing of the positron swarm occurs due to preferential loss at the front of the group leading to a major reduction (NDC) for the bulk drift velocity. One such example is water vapour [28], which is critically

important for applications of positrons in medicine. Assuming that a set of cross sections is sufficiently complete, we may proceed to model tracks of positrons in water vapour allowing also for assessment of nanodosimetry [29].

One should be aware that some of the critical devices in positron physics contain gas to reduce the energy of positrons, below the threshold for Ps formation, and then to further cool them so that the outgoing beams might have a very narrow energy spread. the Penning-Malmberg-Surko trap is usually separated to three stages, with pressures ranging from $10^{-3}$ Torr to $10^{-5}$ Torr, with pure $N_2$ at the front and mixture of $N_2$ and $CF_4$ in the last stage [30,31]. We have been able to apply the code originally developed for electron swarms (and tested against all known benchmarks) to model the Surko trap [32]. In figure 3 one can see the development of the distribution function from a single beam, through to multiple beams (due to inelastic collisions with electronic excitations), and to gradual development of the low energy distribution which becomes dominant and eventually decays to the Maxwell Boltzmann distribution at room temperature [33]. This is fully analogous to the equilibration of electron swarms with initial beam, followed by Frank Hertz like effects during the first collisions and subsequent development of a broad energy distribution function demonstrating also that interpretation of the experiment using swarm phenomenology is appropriate (including of course a good set of cross sections). Having this tool it became possible to determine other aspects of trap operation: losses, optimum choice of potential drops and geometry. It led to some new proposals such as the idea of S. Marjanović for the inversion of the gases, whereby $CF_4$ would be used at the trap front and with the mixture still at the last stage, with lower potential drops that would help avoid Ps formation and allow efficiencies of up to 90%.

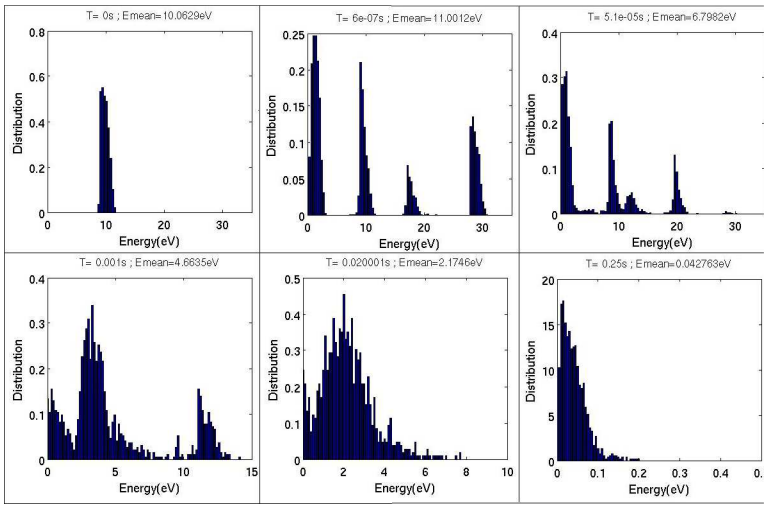


**Figure 3**. Temporal development of the energy distribution function in a positron trap [33].

A large number of elastic collisions, which happen during thermalization, leads to an expansion of the positron swarm in the trap. For many applications, however, increased density is required and thus additional narrowing in the final stage may be required. For this purpose a rotating wall stage has been developed that may operate in two regimes: single particle [34,35] and plasma regimes. A theory of the former has been provided in reference [36] where viscosity was added to a simple transport equation allowing the experiments to be fitted. In our approach a swarm based Monte Carlo codes has been used with realistic sets for the cross sections [37]. The role of each of the processes has been elucidated, and it is possible to characterise all the salient features of the rotating wall trap. As the system develops with an entire ensemble, it appears that the term single particle rotating wall should be replaced by the swarm regime of the rotating wall.

## 5. Conclusion

The realm of the physics of ionized gases controlled by collisions without a significant effect of the Coulomb interaction between charged constituents, is known as swarm physics. It is in this area that the kinetic phenomena are observed most directly. The tools of swarm physics allow us to cross the path from the elementary microscopic collisional processes all the way to the macroscopic properties of swarms, plasmas and other forms of charged particle ensembles and their applications. It appears that for gas filled systems the phenomenology, tools and data of swarm physics provide the best way

to understand and even optimize the devices and their applications, while crossing the gap between microscopic cross sections and the large scale practical devices.

**References**

[1] Huxley LGH and Crompton RW The drift and diffusion of electrons in gases, John Wiley, New Yourk (1974).
[2] Kumar K, Skullerud H R and Robson R E 1980 *Aust. J. Phys.* **33** 343
[3] Petrović Z Lj, Dujko S, Marić D, Malović G, Nikitović Ž, Šašić O, Jovanović J, Stojanović V and Radmilović-Rađenović M 2009 *J. Phys.* D: *Appl. Phys.* **42** 194002
[4] Robson RE 2006 *Introductory transport theory for charged particles in gases* (World Scientific: Singapore)
[5] Robson RE, White RD and Petrović Z Lj 2005 *Rev. Modern Phys*. **77** 1303
[6] Petrović ZLj, Haddad G and Crompton RW1984 *Aust J Phys* **37** 23
[7] Robson RE, Petrović ZLj, Raspopović ZM and Loffhagen D 2003 *J. Chem. Phys.* **119** 11249
[8] Puač N, Maletić D, Lazović S, Malović G, Đorđević A and Petrović ZLj 2012 *Appl. Phys. Lett.* **101**, 024103
[9] Zhongmin Xiong and Kushner M. 2012 *Plasma Sources Sci. Technol.* **21** 034001
[10] Miletić M, Mojsilović S, Okić Đorđević I, Maletić D, Puač N, Lazović S, Malović G, Milenković P, Petrović Z Lj and Bugarski D 2013 *J. Phys. D: Appl. Phys* accepted
[11] Graves D B 2012 *J. Phys. D: Appl. Phys*. **45** 263001 (42pp)
[12] Šašić O, Dupljanin S, De Urquijo J and Petrović Z Lj 2013 *J. Phys.* D: *Appl. Phys.* **46** 325201
[13] Dujko S, White R D, Petrović Z Lj and Robson R E 2010 *Phys. Rev. E* **81** 046403
[14] Dyatko N A, Napartovich A P, Petrović Z Lj, Raspopović Z R and Sakadžić S 2000 *J. Phys. D: Appl Phys.* **33** 375
[15] Šuvakov M, Ristivojević Z, Petrović ZLj, Dujko S, Raspopović ZM, Dyatko NA, Napartovich AP 2005 *IEEE Trans. Plasma Sci.* **31** 532
[16] Robson RE, Petrović ZLj, Raspopović ZM and Loffhagen D 2003 *J. Chem. Phys.* **119** 11249
[17] Phelps A V and Petrović Z Lj 1999 *Plasma Sources Sci. Technol*.**8** R21
Phelps AV Petrović ZLj and Jelenković B M 1993 *Phys. Rev*. E **47** 2825
[18] Marić D, Malović G and Petrović Z.Lj. Plasma *Sources Sci. Technol*. **18** (2009) 034009
[19] Riegler W and Lippmann C. 2004 *Nucl. Instr. Meth. A* **518** 86
[20] Bošnjaković D, Petrović ZLj and Dujko S, in Proceedings of XVIII International Symposium on Electron-Molecule Collisions and Swarms, 19-21 July 2013, Kanazawa, Japan, p. 44
[21] Makabe T and Petrović Z Lj 2006 *Plasma Electronics* (New York: Taylor and Francis)
[22] Dujko S, Markosyan A, White R D and Ebert U 2013 *J. Phys. D: Appl. Phys*. Submitted
[23] Campbell L and Brunger M J 2013 *Plasma Sources Sci. Technol.* **22** 013002
[24] Charlton M 2009 *J. Phys.: Conf. Ser*. **162** 012003
[25] Marler J. P., Surko C. M., 2005 *Phys Rev* A **72** 062713
[26] Surko C M, Gribakin G F and Buckman S J 2005 *Journal of Physics B* **38** R57-R126
[27] Makochekanwa C, Banković A, Tattersall W, Jones A, Caradonna P, Slaughter D S, Sullivan J P, Nixon K, Brunger M J, Petrović Z Lj, Buckman S J, 2009 *New J. Phys*.**11** 103036
[28] Banković A, Dujko S, White R D, Marler J P, Buckman S J, Marjanović S, Malović G, García G, Petrović Z Lj, 2012 *New Journal of Physics* **14** 035003
[29] Petrović Z Lj, Marjanović S, Dujko S, Banković A, Malović G, Buckman S, Garcia G, White R, Brunger M 2013 *Appl. Radiat. Isotopes* Available online doi: 10.1016/j. apradiso.2013.01.010
[30] Greaves R G and Surko C M 2002 *Nuc. Inst. Meth. in Phys. Res. B* **192** 90
[31] Sullivan J P, Jones A, Caradonna P, Makochekanwa C and Buckman S J 2008 *Rev. Sci. Instrum.***79** 113105
[32] Marjanović S, Šuvakov M, Banković A , Savić M, Malović G, Buckman S J and Petrović Z Lj 2011 *IEEE Trans. Plasma Sci.* **39** 2614

[33] Marjanović S, Šuvakov M, Banković A and Petrović Z Lj 2011 unpublished
[34] Cassidy D B, Deng S H M, Greaves R G and Mills Jr A P 2006 *Rev. Sci. Instrum.***77** 073106
[35] Greaves R G and Moxom J M 2008 *Phys. Plasmas* **15** 072304
[36] Isaac C A, Baker C J, Mortensen T, van der Werf D P and Charlton M 2011 *Phys. Rev. Lett.* **107** 03320
[37] Marjanović S *et al.* 2012 unpublished

CEAMPP 2013

3rd National Conference on Electronic,
Atomic, Molecular and Photonic Physics
Belgrade, Serbia, August 25th, 2013

# CONTRIBUTED PAPERS

&

# ABSTRACTS OF INVITED LECTURES AND PROGRESS REPORTS

University of Belgrade

Faculty of Physics

Editors
B.P. Marinković, G.B. Poparić

University of Belgrade, Faculty of Physics,
Belgrade, Serbia

# A microscopic model for time response of Resistive Plate Chambers

D. Bošnjaković[1], Z. Lj. Petrović[1] and S. Dujko[1,2]
[1] *Institute of Physics, University of Belgrade, Pregrevica 118, 11080 Zemun, Serbia*
[2] *Centrum Wiskunde & Informatica (CWI), P.O. Box 94079, 1090 GB Amsterdam, The Netherlands*
e-mail: sasa.dujko@ipb.ac.rs

**Abstract.** We present a new microscopic approach in modeling of Resistive Plate Chambers (RPCs) which is based on the Monte Carlo method. RPCs are used in many high energy physics experiments for timing and triggering purposes [1]. Due to their excellent timing properties they are also considered for use in next generation medical imaging devices. These detectors consist of one or several gas gaps between electrodes of high resistivity. Electrodes of highly resistive material, such as glass or bakelite, are used for suppression of spark formation. RPCs can be operated in avalanche or streamer mode with timing resolution down to 50 ps and efficiencies of up to 95% for single-gap configuration.

In our microscopic model, individual electrons are traced in a typical Monte Carlo fashion. Cross sections sets for electron collisional processes in $C_2H_2F_4$, iso-$C_4H_{10}$ and $SF_6$ (typically used in the RPC gas mixtures) were assembled from available sources. In addition, a new cross sections set for $C_2H_2F_4$ was recently developed by our group [2]. Electron transport coefficients, required for comparison with macroscopic probabilistic models of these detectors, were obtained from solution of the non-conservative Boltzmann equation [3]. Results showed remarkable similarity of ionization rate calculated using our cross section for $C_2H_2F_4$ with that calculated by using cross sections from MAGBOLTZ 8.9 [4].

Beside electron avalanche model, implementation of primary ionization and geometrical constraints was also required. The primary ionization, made by a high-energy particle travelling through the detector, was included using a well known probability model with the available data for mean distance between electron clusters and cluster size distribution, assuming minimum ionizing particles. Finally, we present our results for timing resolution and efficiency which were calculated for a specific timing RPC geometry (0.3 mm gas gap, one glass and one metallic electrode) with different cross section sets and primary ionization models. Contrary to a probabilistic model [5], results show that effective ionization rate is not the sole factor which determines the timing resolution and that the cross section set as a whole is also a determining factor for RPC parameters.

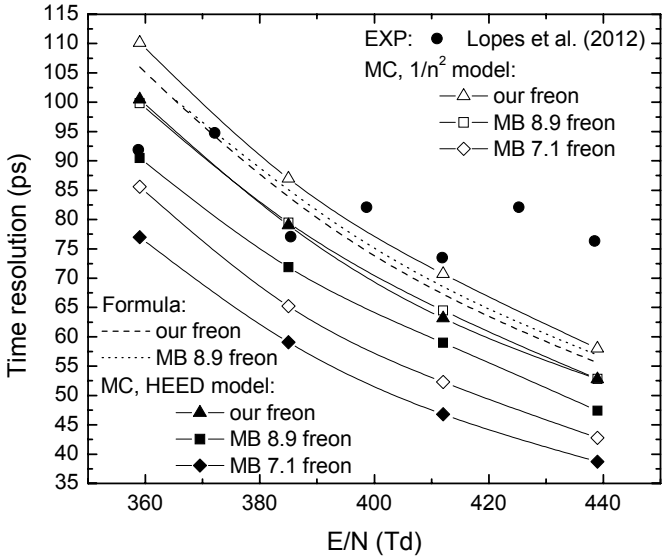


*Timing resolutions for different cross section sets and primary ionization models. Comparison with experimental values from Lopes et al. (2012).*

[1] P. Fonte, IEEE Trans. Nucl. Sci. **49** 881 (2002).
[2] O. Šašić, S. Dupljanin, J. de Urquijo and Z.Lj. Petrović, J. Phys. D **46** 325201 (2013).
[3] S. Dujko, R.D. White, Z.Lj. Petrović and R.E. Robson, Phys. Rev. E **81** 046403 (2010).
[4] S. Biagi, Nucl. Instr. and Meth. A **421** 234 (1999).
[5] W. Riegler and C. Lippmann, Nucl. Instr. and Meth. A 518 **86** (2004).